ASYMETRIC BEHAVIOR OF A DROP UPON IMPACT ONTO A SURFACE

HAMED ALMOHAMMADI

A THESIS SUBMITTED TO

THE FACULTY OF GRADUATE STUDIES

IN PARTIAL FULFILLMENT OF THE REQUIRMENTS

FOR THE DEGREE OF

MASTER OF SCIENCE

GRADUATE PROGRAM IN MECHANICAL ENGINEERING

YORK UNIVERSITY

TORONTO, ONTARIO

SEPTEMBER 2016

Abstract

In this thesis, a systematic study was performed to understand drop impact onto hydrophilic and hydrophobic moving surfaces. Different systems (combination of liquids, surfaces, and drop impact conditions) were examined. Wide range of normal drop and surface velocities were studied; such normal and tangential velocity ranges are not available in systems where a drop impacts at an angle relative to a surface. The asymmetric nature of drop spreading on moving surfaces was elucidated. A model that for the first time is able to mathematically predict the time evolution of such asymmetric spreading was provided. Furthermore, a new model was developed to determine the splashing threshold of the drop impact onto a moving surface. The model is capable of describing the azimuthally different behavior of splashing. The effect of liquid viscosity on drop splashing was clarified. A comprehensive regime maps of drop impact outcome on a moving surface was provided.

This thesis is dedicated to my parents,

Yavar and Narges.

Acknowledgment

First of all, I am deeply grateful to my supervisor, Prof. Alidad Amirfazli, for his endless supports and invaluable guidance. Working under his supervision, I learned how to think systematically and communicate as a research scientist. I am sure that these learnings will help me not only in the rest of my career, but also in my professional life.

I am also very grateful to Dr. Huanchen Chen for very helpful technical discussions. In addition, I would like to acknowledge Mr. Mohammad Al Ramahi for the design of the experimental setup.

I am grateful to my family, especially Mom and Dad, for their unconditional love and supports.

TABLE OF CONTENTS

LIST OF TABLES

LIST OF FIGURES

Chapter One

Introduction

1.1 Background and Motivation

Drop impact onto a surface is of importance in many applications including printing (e.g. inkjet printing, electronic board) [1–3], painting and coating (e.g. pharmaceutical, agricultural, rail industry, cosmetic, textile, and food) [4–7], and cooling of the hot surfaces (turbine blades, semiconductor chips, and electronic devices) [8,9]. However, there are some instances where drop impact results in undesirable outcomes like ice accumulation on power lines and aircraft [10,11]. As such, to get drops do what is desired, we need to understand how a drop impacts onto a surface and, if it is possible, quantify its behavior.

Upon normal drop impact onto a horizontal surface, various outcomes can be seen (see below) [12–15]. The impact condition (i.e. drop normal velocity, and drop size) [15], liquid (i.e. density, viscosity, and surface tension) [16–20], surface (i.e. roughness and wettability) [18,21–23], and surrounding medium [19] are the parameters which can affect the outcome of the drop impact. The following are the outcomes of drop normal impact onto a surface: prompt splashing, corona splash, receding breakup, rupture, temporary dry spot in a lamella, partial rebound, complete rebound, and deposition (Figure 1.1) [24]. The description of each outcome is provided in the following as this information sheds light on better understanding of the other systems of drop impact:

Splashing: this behavior can be seen during radially expanding of the liquid film over the surface. There are two forms of splashing:

a) Prompt splash: where tiny droplets are generated directly at contact line of the lamella.
b) Corona splash: in this type of splashing lamella lifts off the surface and subsequently detaches away from the surface.

The splashing probability increases as the drop velocity (drop kinetic energy) increases or surface tension (surface energy) decreases [15]. However, the role of viscosity (involved in viscous forces) on drop splashing is not clear yet; some studies show that increase in viscosity promotes splashing [16,19], while others have found opposite trend [17,25,26]. The role of viscosity on splashing will be addressed in this thesis.

Receding break up: this refers to the uneven motion of a contact line when the lamella recedes from its maximum spreading. Decrease in the liquid viscosity or increase in normal drop velocity promotes receding break up [15].

Rupture: this behavior refers to the formation and appearance of the holes at liquid film. The air bubbles, which are trapped between the impacting drop and the surface, result in such holes [27].

Temporary dry spot: in this condition there are air bubbles which are trapped between the liquid film and surface, but they do not appear as a dry spots. The air bubbles either disappear without any changing in lamella morphology or collapse and results in the appearance of singular jets (see Figure 1.1) [28,29].

Partial and complete rebound: The partial rebound refers to a condition where, in the receding phase, some portion of the lamella detach from the rest of the liquid and subsequently leave the surface; while in the complete rebound, whole of the liquids leaves the surface. The chance of partial rebound becomes higher with an increase in the drop normal impact velocity or the

receding contact angle of the liquid on the surface [15]. It also is found that in the case where receding contact angle is >100° and 25 < We_n < 585 ($We_n=\rho V_n^2 D_0/\sigma$, where ρ is the liquid density, D_0 is the drop diameter, and σ is the liquid surface tension), the water drops rebound completely [23,30].

Deposition: this refers to a condition where, after drop impact onto a surface, the liquid radially spreads over the surface until the maximum diameter is reached; then the contact line of liquid film either recedes or pins.

As it is clear, for the outcomes of receding breakup, rupture, temporary dry spot in a lamella, partial rebound, complete rebound, and deposition drop is in spreading phase at the initial time (see last 7 panels in Figure 1.1). The spreading ends with reaching of maximum spreading diameter. Therefore, one can make a conclusion that upon normal drop impact onto a surface drop either spreads or splashes at initial time [31].

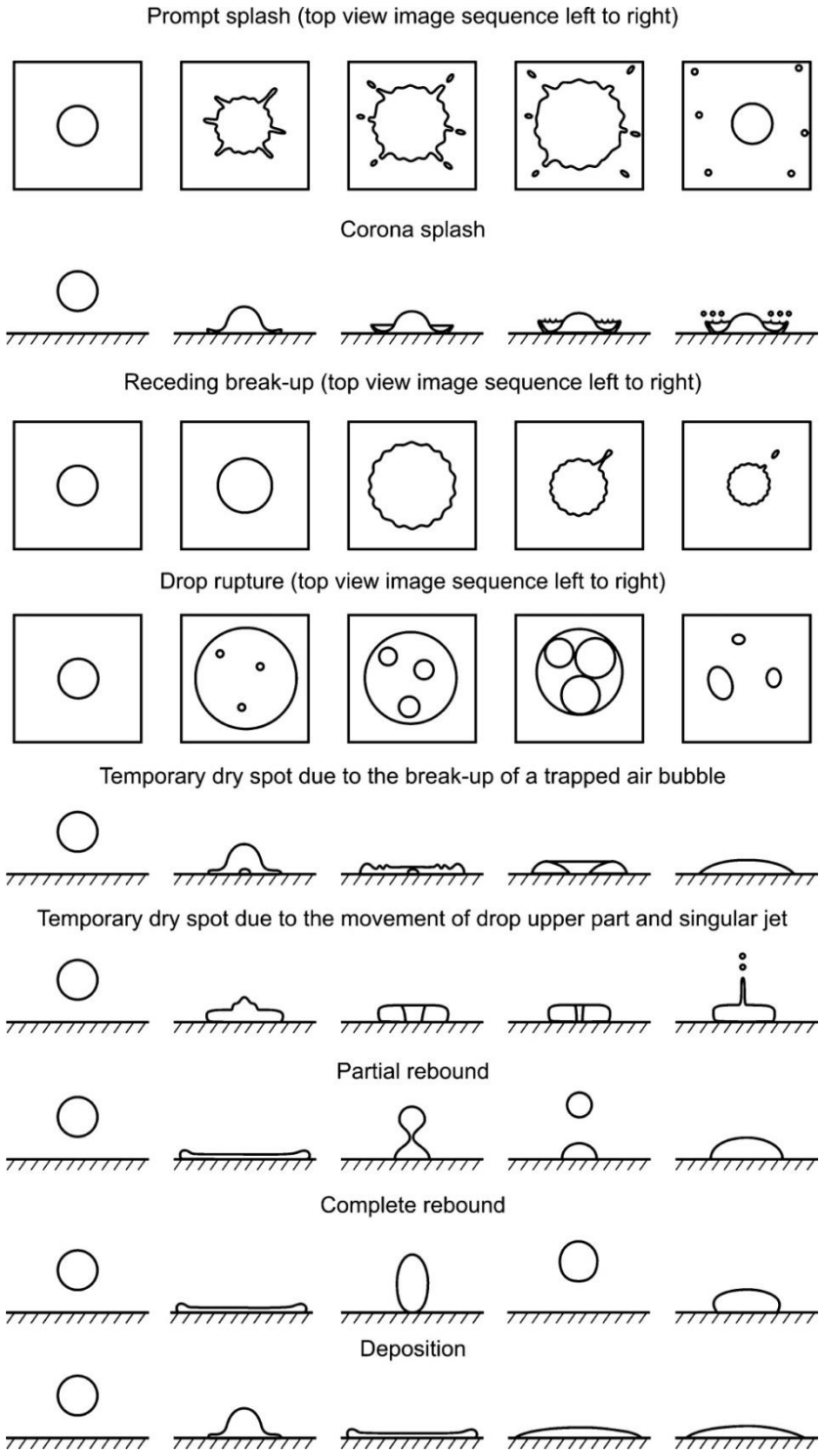

Figure 1.1: Outcomes of drop normal impact on a horizontal surface. The panels should be read from left to right [24]. Reprinted with permission from (Grishaev, V.; Iorio, C. S.; Dubois, F.; Amirfazli, A. Complex Drop Impact Morphology. *Langmuir* **2015**, *31*, 9833–9844.). Copyright (2016) American Chemical Society.

There are many experimental and numerical studies in the literature to describe both qualitatively and quantitatively the various outcomes (as introduced before) of normal drop impact onto a horizontal surface (see review works [12–14] for more details). However, in many of the applications (mentioned earlier) drop impacts onto a surface in a condition where the impact has both normal and tangential velocities and only a few works have been done in this area. Both normal and tangential velocities for impact can be seen in systems including drop impact onto a moving surface, oblique drop impact onto a surface, and drop impact onto an inclined surface (see Figure 1.2). As such, the fundamental understanding of the process is still in its infancy and the answer to a question of how tangential velocity changes the behavior than that of the only normal impact is not clear yet. The need for further works to understand the effect of tangential velocity on drop impact is also highlighted in the recent review work of drop impact phenomena (published in 2015 [13]). Here, we use the system of normal drop impact onto a moving surface to study the effect of tangential velocity on drop impact process. The first advantage of this system is that one can study the role of the tangential velocity in wide velocity range; the other advantage is the ease of controlling each of the normal and tangential velocities separately.

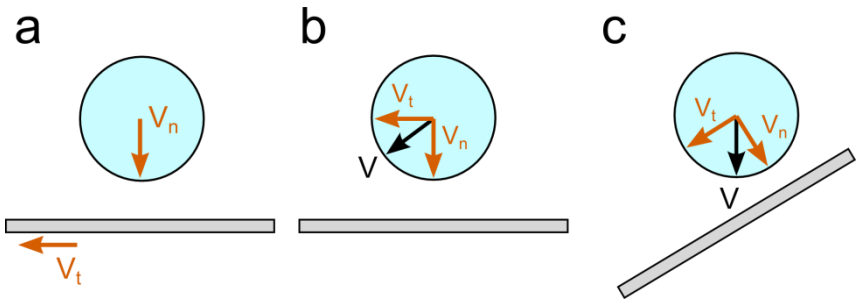

Figure 1.2: Schematic view of the (a) normal drop impact onto a moving surface, (b) oblique drop impact onto a horizontal surface, and (c) drop impact onto an inclined surface. It is assumed that surface moves with V_t.

To date, most of the literatures have been focused on whether drop spreads or splashes at upstream or downstream upon impact onto a moving surface [26,32–36]. It was found that for drop impact onto a moving surface, there are asymmetric outcomes including spreading in one side of the drop and splashing at the other side of the drop [26,32–34]. As such, if the drop impact conditions led to spreading for a stationary surface (Figure 1.3a), surface movement can change the spreading behavior to splashing at the side where the lamella moves at the opposite of direction of the surface motion (Figure 1.3c) [26,32,34]. Also, if drop impact conditions are such that drop would splash on a stationary surface (Figure 1.3b), movement of the surface can suppress the splashing at the side where the lamella moves in the direction of the surface motion and changes it to spreading (Figure 1.3c) [26,32–34]. The same observations are made for drop impact onto an inclined surface [34,37]. Aboud et al.[32] recently found that, upon drop impact onto a moving hydrophobic surface, an additional behavior of stretch rebounding was observed. Stretch rebounding refers to complete rebound of a droplet which is stretched by the surface motion. However, the process of such stretch rebounding was not investigated in details. It is also found that using hydrophobic surface promotes splashing for drop impact on a moving surface.

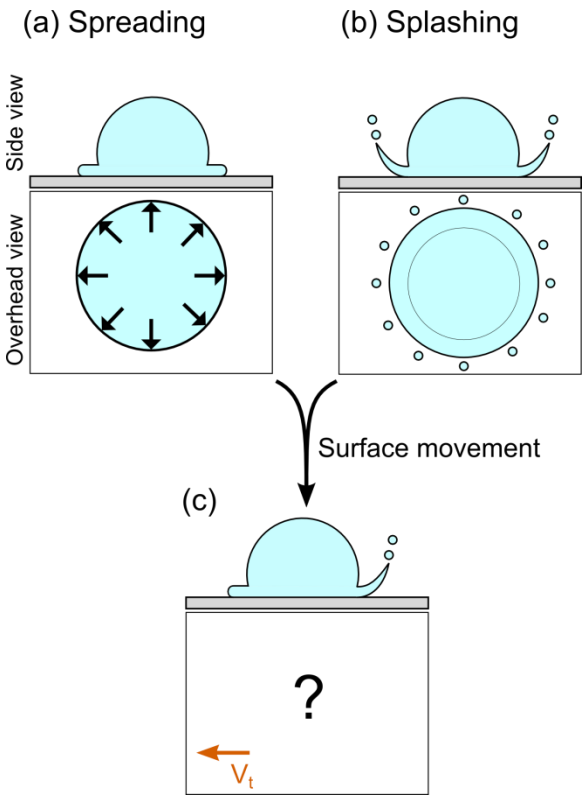

Figure 1.3: Schematic view of drop (a) spreading, and (b) splashing over a stationary surface. (c) Shows schematically one side splashing of the drop over a moving surface. Surface moves from right to left.

It is clear that a few studies have been conducted to investigate drop impact onto a moving surface. The lamella development (how drop lamella spreads or recedes) that is of a fundamental importance for drop impact onto a surface is not studied yet. The understanding in literature, i.e. 2D asymmetric behavior for drop impact onto a moving surface, is highly questionable, since the direction of the lamella velocity along the lamella contact line (which is radially outward) differs azimuthally from the surface velocity direction, i.e. it is 3D asymmetric. This issue is from the fact that most of the works so far have been performed only from the side view observations. As such, if the lamella is azimuthally asymmetric (3D asymmetric), following are the issues which should be addressed:

- How surface motion (i.e. tangential velocity) changes the lamella development (i.e. lamella expanding, pinning, and recoiling process) from that of stationary one? The answer can also help with understanding the wettability effects (e.g. how stretch rebounding occurs).
- Having understood the lamella development of drop, how parameters of drop and surface velocities, surface wettability, and liquid viscosity affect the lamella shape? Or, how is the time evolution of the liquid film outline upon drop spreading on a moving surface at various drop impact conditions? The answer will be a relation which is capable to describe asymmetric spreading seen when a drop impact onto a moving surface.
- Is the drop splashing on a moving surface azimuthally asymmetric as well? If yes, there will be need to study both qualitatively and quantitatively drop splashing on a moving surface.
- How liquid viscosity affects splashing behavior of a drop upon impact onto a surface? As mentioned before, this issue is not understood yet for drop impact onto a stationary surface, as a most simple and basic format of drop impact.

1.2 Objectives of this Thesis

In this thesis, a systematic study was performed to understand drop impact onto hydrophilic and hydrophobic moving surfaces. More than 450 different systems, i.e. combination of liquids, surfaces, and drop impact conditions, were examined. Considering the mentioned gaps, the goals of this thesis are to:

1. Identify all of the possible outcomes of the drop impact onto a moving surface

2. Understand the azimuthal development (expanding, pinning, and recoiling process) of the lamella upon drop impact onto a moving surface
3. Understand how parameters of drop and surface velocities, surface wettability, and liquid viscosity affect the lamella shape; and, develop a model to predict the drop spreading outline over a moving surface
4. Understand the drop splashing over a moving surface and develop a model to predict the splashing behavior all around the lamella contact line
5. Conduct a preliminary investigation on the effect of liquid viscosity on splashing behavior of a drop upon impact onto a stationary surface

It should be noted that this thesis focuses on investigation of drop impact onto moving hydrophilic and hydrophobic surfaces; the surfaces with the same roughness are used in this study. When surfaces with different roughness are involved, the outcome of the drop (like splashing) will be affected. Furthermore, the surface elasticity or extreme wettabilities effects (such as superhydrophobic or superhysrophilic surfaces) were not studied in this study.

All of the liquids which are used in this study are Newtonian fluid. For the non-Newtonian fluid, the viscosity is not constant as such the behavior can be more complex during the impact process. Understanding how surrounding gas pressure affects the drop impact process is beyond the scope of this thesis. In addition, here we mainly focused on the spreading and splashing behaviors of the drop upon impact onto a moving surface; as such the behaviors like what happens with the drop after it rebounds at very high surface velocity is not discussed.

1.3 Thesis outline

The writing of this thesis is organized around two papers that are either submitted or in the process of submission now, as well as one ongoing work; each of these forms one chapter in this

thesis. As such, each part will have its more focused introduction, motivation, and literature review. Below the outline of this thesis is explained:

Chapter 2: in this chapter, we will explain the azimuthal development (expanding, pinning, and recoiling process) of the lamella upon drop impact onto a moving surface. Effect of the parameters, like wettability, on lamella development will be discussed. Different form of splashing for drop impact onto moving surface will be reported. A model will be developed to predict the splashing behavior all around the lamella contact line. We will discuss the effect of viscosity on drop impact process and outcomes for moving surfaces. Comprehensive regime maps for the drop impact onto both hydrophilic and hydrophobic surfaces will be presented.

Chapter 3: We will study the spreading behavior of a drop upon impact onto a moving surface. The effect of the normal and tangential velocities and surface wettability on drop spreading will be discussed. A model will be developed to mathematically predict not only the maximum spreading of lamella, but also time evolution of the lamella. The model prediction will be validated with experimental data.

Chapter 4: In this chapter, the effect of the liquid viscosity on splashing behavior of a drop upon normally impact onto a stationary surface will be discussed. To date understanding in tem of role of viscosity on drop splashing will be explained. The possible reasons on why there is a low agreement viscosity effect on drop splashing will be discussed. Finally, our experimental results and discussion about the effect of viscosity on splashing will be presented.

Chapter Two

Understanding the drop impact onto moving hydrophilic and hydrophobic surfaces[1]

2.1 Introduction

It is important to understand the behavior of drop impact onto a surface due to its various applications such as inkjet printing [1,2], spray coating (rail industry [6,7]) and cooling (turbine blades [9]). There are many experimental and numerical studies in the literature on the drop impact onto a stationary surface [12–14]. However, many of the above applications involve drop impact onto a moving surface and only a few works have been done in this area.

In the case of the drop impact onto a stationary surface, two stages can be recognized: First, when, after contact with the surface, the drop moves vertically down and the liquid radially spreads over the surface until it reaches the maximum diameter, D_{max} (see expansion in Figure 2.1a); second, after the lamella reaches its maximum spreading which results in either receding or pinning of contact line (retraction, Figure 2.1a). Drop shows different behaviors during these two stages [15,24].

[1] This chapter is submitted to Soft Matter. Authors: Hamed Almohammadi and Alidad Amirfazli

In the first stage (Figure 2.1a), where the kinetic energy of the droplet is high, three main outcomes are observed: spreading, prompt splashing and corona splashing (at very high speeds disintegration of drop is also possible). Spreading refers to the radial expansion of the lamella over the surface without any detachment. Prompt splashing happens when tiny droplets detach from the advancing contact line of the lamella; while corona splashing occurs when the lamella lifts off the surface which subsequently breaks up into tiny droplets. Depending on the drop velocity, diameter, surface tension and viscosity [16–19], surface roughness [18,21] and surrounding gas [19] the outcomes differ.

In the second stage (Figure 2.1a), the kinetic energy of the drop has mainly dissipated by viscous and surface forces. The lamella may or may not start to recede from its maximum spread. The amount and way of the receding, which depends on impact conditions, liquid [20] and especially surface [22,23] parameters, determine the final outcome. The following outcomes are observed: deposition (with or without receding), receding breakup, partial rebound, and complete rebound.

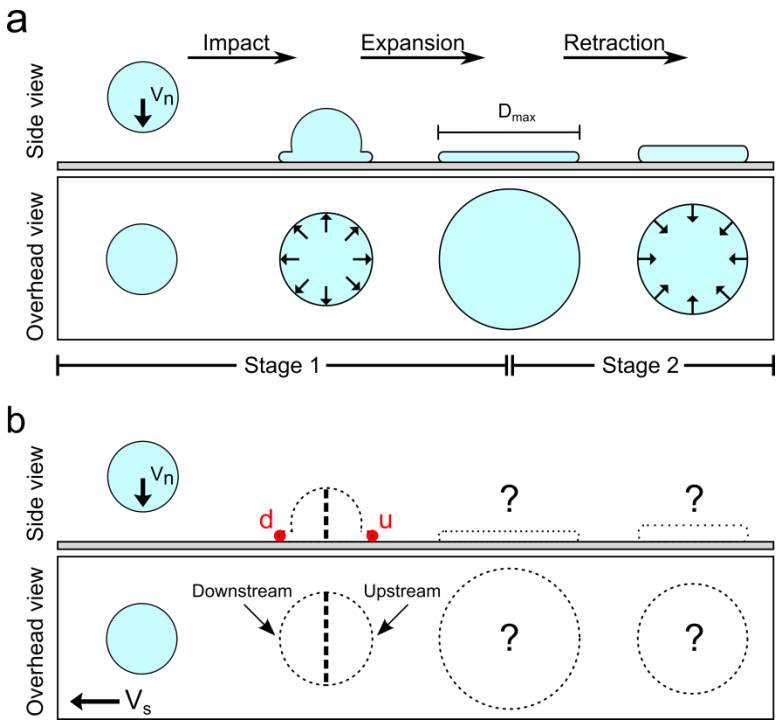

Figure 2.1: Schematic view of the lamella development upon drop impact onto a (a) stationary, and (b) moving surfaces. Dashed line shows the upstream and downstream boundary. Dotted lines show the lamella development when there is no movement of the surface.

The question is how a drop behaves upon impact onto a moving surface (Figure 2.1b)? A few studies have been done to address this question [26,32–36]. It was found that aside from the usual symmetric spreading and splashing, for drop impact onto a moving surface, one can observe asymmetric outcomes like spreading in one side of the drop (downstream in Figure 2.1b) and splashing at the other side of the drop (upstream in Figure 2.1b) [26,32–34]. For example, if drop impact conditions are such that drop would splash on a stationary surface, movement of the surface can suppress the splashing at downstream and change it to spreading [26,32–34]. Also, if the drop impact conditions led to spreading for a stationary surface, surface movement can change the spreading behavior upstream to splashing [26,32,34]. Based on such observations, Bird et al. [26] developed a model for splashing of a drop impacting onto a moving surface using

a 1D axisymmetric analysis, i.e. considering the lamella and surface velocities only at two points at the upstream and the downstream (see points *u* and *d* in Figure 2.1b):

$$We_n Re_n^{1/2}(1-kRe^{-1/2}V_s/V_n)^2>K \quad (2.1)$$

where V_s and V_n are the surface and drop velocities, respectively. To predict the splashing at *downstream* or *upstream*, surface velocity should be used with *positive* or *negative* values, respectively; We_n is the normal Weber number ($We_n=\rho V_n^2 D_0/\sigma$, where ρ is the liquid density, D_0 is the drop diameter, and σ is the liquid surface tension); and Re_n refers to the normal Reynolds number ($Re_n=\rho V_n D_0/\mu$, where μ is the liquid dynamic viscosity). In addition, k and K are the constants of the order of one, and much higher than one, respectively. Bird et al. [26] reported good agreement between their experimental results and that of Eq. (2.1). There are two issues however that needs attention. In Ref. [26] only one liquid (ethanol) was used to validate the Eq. (2.1), so the question remains, if viscosity or surface tension or surface wettability can make a difference? Secondly, the model was based on a 1D concept, but as discussed above the spreading is asymmetric azimuthally (see also below).

Very recently, Aboud et al. [32] observed if a hydrophobic surface is used, the splash threshold is lowered compared to a hydrophilic surface. In addition, they found that, upon drop impact onto a moving hydrophobic surface, an additional behavior of stretch rebounding is observed. Stretch rebounding refers to complete rebound of a droplet which is stretched by the surface motion. However, the process of such stretch rebounding was not investigated in detail.

Most of the works so far have focused on whether drop spreads or splashes at upstream or downstream upon impact onto a moving surface. However, since most of these works have been performed only from the side view observations, it is not clear whether the lamella is asymmetric with respect to the line between upstream and downstream (see dashed line in Figure 2.1b), or it

is asymmetric azimuthally which cannot be observed from side view. The latter arises from the fact that the direction of the lamella velocity along the lamella contact line (which is radially outward) differs azimuthally from the surface velocity direction (which is from left to right; Figure 2.1b). If the lamella is azimuthally asymmetric, two questions will be raised: first, how is the lamella development (i.e. lamella expanding, pinning, and recoiling process) on a moving surface? Understanding the lamella development can also help with understanding the wettability effects (e.g. how stretch rebounding occurs). Second, is the drop splashing on a moving surface azimuthally asymmetric? If yes, then using a 1D model (like Eq. 2.1) to predict splashing over moving surface will be limited only to two points of *u* and *d* (see Figure 2.1b); this means that to date understanding is limited to only ~0.6% (2/360) portion of the lamella contact line (each point considered as 1˚ span azimuthally). Therefore, there will be a need to develop a model to predict the splashing behavior around the lamella contact line.

Taken all together, it is clear that significantly fewer studies have been conducted to investigate drop impact onto a moving surface. Almost all of existing works did not consider the details of lamella development that is a fundamental issue for drop impact onto a surface. In addition, the predication of the splashing behavior is based on the two points of *u* and *d* (Figure 2.1b), which does not comply with the practical meaning of splashing as understood in the literature. Therefore, in this chapter we provide a systematic study of drop impact onto moving hydrophilic and hydrophobic surfaces for different liquids. We will consider the azimuthal development (expanding, pinning, and recoiling process) of the lamella. A model is developed to predict the splashing behavior all around the lamella contact line. For the first time, we will discuss the effect of viscosity on drop impact process and outcomes for moving surfaces. Comprehensive regime maps for the drop impact onto both hydrophilic and hydrophobic surfaces will be

presented. As such, objectives (1,2, and 4; which are stated in Chapter 1) will be addressed in this section.

2.2 Methods and materials

A schematic view of the experimental setup is shown in Figure 2.2. The setup consists of three main parts: drop generation, moving surface, and recording equipment.

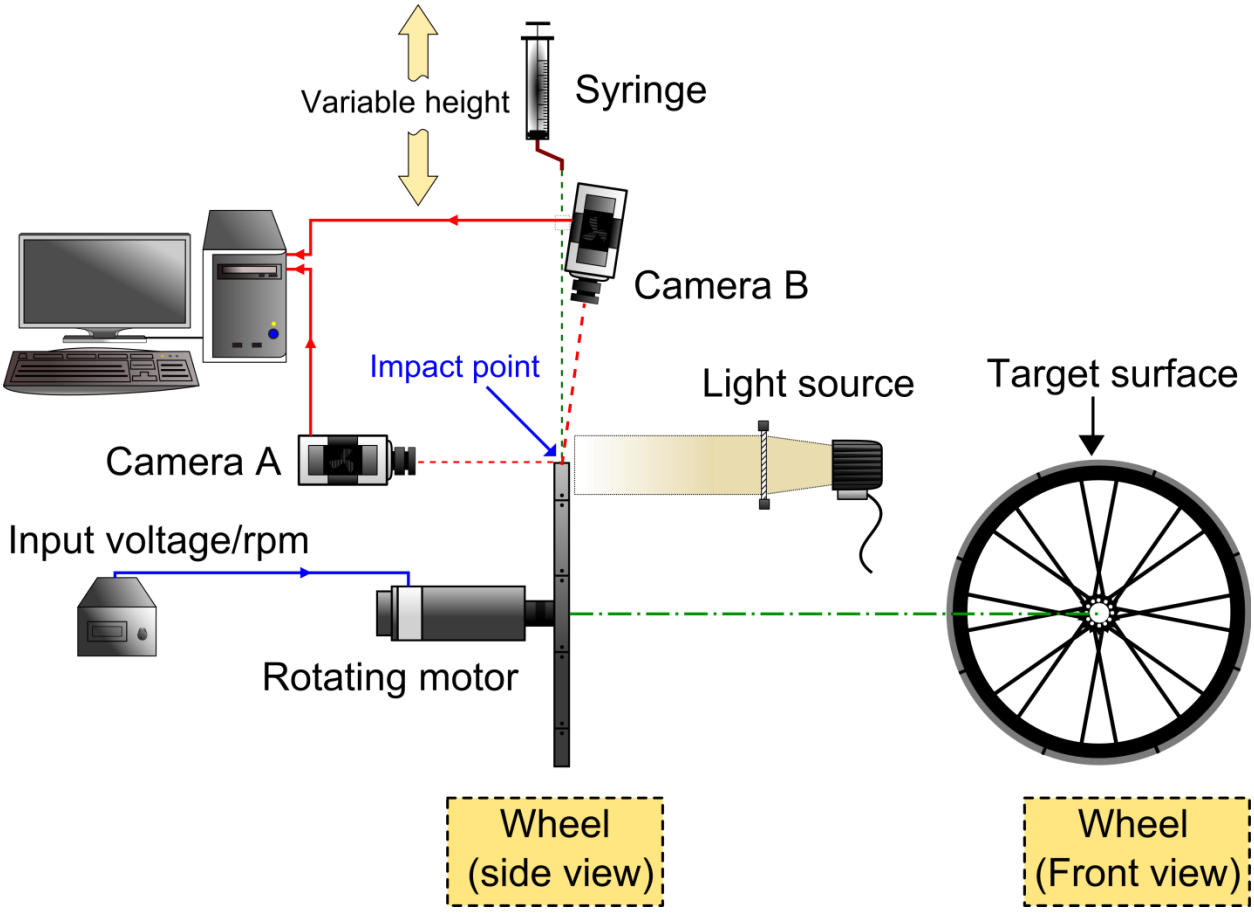

Figure 2.2: Schematic of the experimental setup

Drop generation: To generate drops a syringe-needle system was used. Drops with diameter of D_0=2.5±0.1 mm were released from different heights above the target surface to generate drop velocities from 0.5 to 3.4 m/s. All of the experiments were done at room temperature (20˚C). Mixtures of the water and glycerol with approximately the same surface tension and density, but different viscosities were used as the working fluids (see Table 2.1). The focus was on liquids with viscosities in the range of $\mu/\rho \lesssim 4$ cSt which is referred as a low viscous liquids in the literature (in the context of drop impact). For low viscous liquids, it is well known that increase of the viscosity enhances the splashing on stationary surfaces [16,18,19].

Table 2.1: Physical properties of the working fluids

Liquid name	Percentage of glycerol (wt %)	Density ρ (kg/m^3) [38]	Surface tension σ (mN/m) [38]	Dynamic viscosity μ (mPa.s) [39]
Water	0	998.2	71.7	1.005
Mixture 1	24	1057.2	70.6	2.025
Mixture 2	42	1104.7	69.2	4.106

Moving surface: Two surfaces with different wettabilities were used as target surfaces. The hydrophilic surface was a stainless steel surface with advancing and receding contact angles of 89±1˚ and 34±2˚, respectively. Teflon coated stainless steel with advancing contact angle of 123±1˚ and receding contact angle of 109±1˚ was used as the hydrophobic surface. To fabricate Teflon coated surfaces, a solution containing FC-75 and Teflon (5:1 (v/v) FC-75, 3-M/Teflon AF, Dupont) was prepared and spray coated over the cleaned (with DI water and acetone)

stainless steel. A surface profilometer was used to quantify the surfaces' roughness; where Sq (root mean square height of the surface) was measured to be 112±20 nm for hydrophobic and 69±4 nm for hydrophilic surfaces (see Supporting Information for details). Considering Ref. [19], it will be reasonable to assume the similar roughness for both surfaces.

The surfaces were mounted on a rotating large wheel (Dia. 56.9 cm). The wheel was rotated at various rotational velocities by changing the input voltage of a motor (see Figure 2.2). Wide range of rotational speeds, which gives linear velocity in the range of 0 to 17 m/s, was used. We assumed the target surface as a moving horizontal surface. Note the justification of this assumption is available in the Appendix A.

Recording: The experiments were recorded from both side and overhead. High speed phantom cameras were used at 5,000 and 10,000 fps from overhead and side views, respectively.

2.3 Results and discussion

Drop impact onto both stationary and moving hydrophilic surfaces are presented in Figure 2.3. For the stationary surface, upon impact, drop expands radially over the surface until it reaches the maximum diameter (D_{max}). After reaching the maximum diameter, lamella recedes from its maximum spreading (Figure 2.3a). On the moving surface, drop spreads asymmetrically over the surface which results in an elongated and asymmetric outline (Figure 2.3b). The lamella spreads more in the direction of surface movement compared to that of a stationary surface. Looking at lamella width, during the spreading, the lamella grows until the maximum width is reached; then, it starts to recoil (Figure 2.3b).

Considering the context of the drop impact onto a stationary surface, the time corresponding to D_{max} is expressed as t_{max}; for drop impact onto a moving surface we defined the t_{max} as a time when the lamella reaches its maximum width (Figure 2.3 third row). The maximum width line is considered as a boundary between the upstream and downstream regions. The behavior of the drop impact onto a moving surface, similar to an impact onto a stationary surface can be studied in two phases: (i) lamella development before reaching the maximum width ($t \leq t_{max}$), and (ii) after reaching the maximum width ($t > t_{max}$).

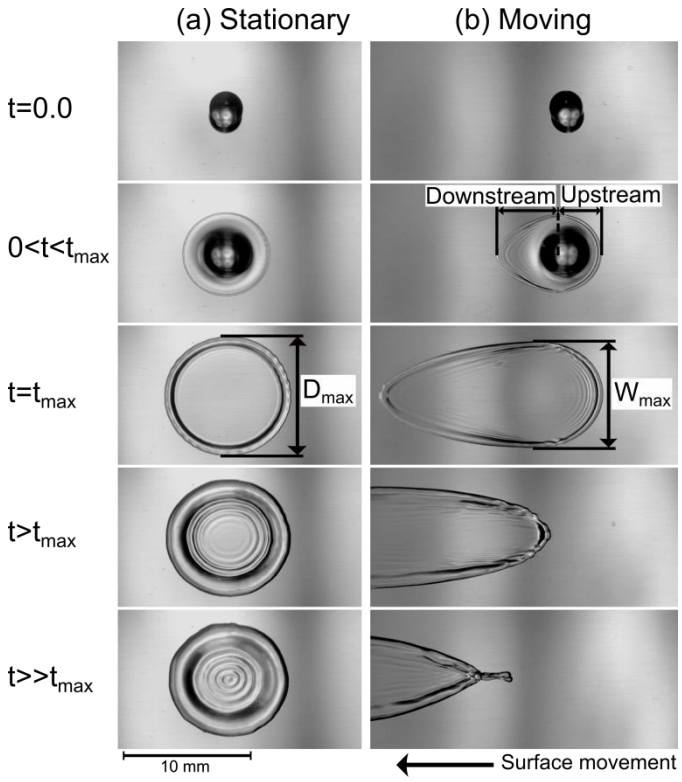

Figure 2.3: Overhead view of the drop impact onto a (a) stationary, and (b) moving hydrophilic surfaces (stainless steel). Drop velocity is V_n=2.01 m/s, and surface velocities are (a) V_s= 0 m/s, and (b) V_s= 5.82 m/s; surface moves from right to left.

2.3.1 Lamella development before tmax

2.3.1.1 Spreading

Spreading of a drop over a moving surface is due to two facts: First, drop's initial kinetic energy; second, momentum transfer from the surface to lamella. The first one leads to lamella expansion around the liquid body of the drop; and the second stretches the lamella in the direction of the surface movement (Figures 2.4a and 2.4c).

Interestingly, we found that the liquid body of drop moves only vertically down after contact with the surface during the spreading process; this can be seen from drop body motion in Figures

2.4a and 2.4c which is along the vertical dashed line. Location of the liquid body is important since the lamella expansion occurs around the drop, as it flattens. The results for various drop impact conditions, surfaces (both hydrophilic and hydrophobic), and various drop viscosities show the same vertical movement for the drop (see Appendix A). It should be noted that the vertical movement of the drop during spreading over the moving surface can be understood by the negligible shear transfer from the surface to the bulk of the drop. In other words, since for tested liquids the momentum transfer only affects the liquid very close to the surface, one do not observe horizontal movement affecting the bulk of the drop (i.e. resulting in remaining of drop apex on a vertical path).

To summarize the general behavior, the asymmetric shape of the lamella can be explained by: (i) initial kinetic energy of the drop impact which leads to expanding of the lamella around the drop, (ii) momentum transfer from the surface which results in stretching of the expanded lamella in the direction of the surface movement. More specific findings for hydrophilic and hydrophobic surfaces are discussed below.

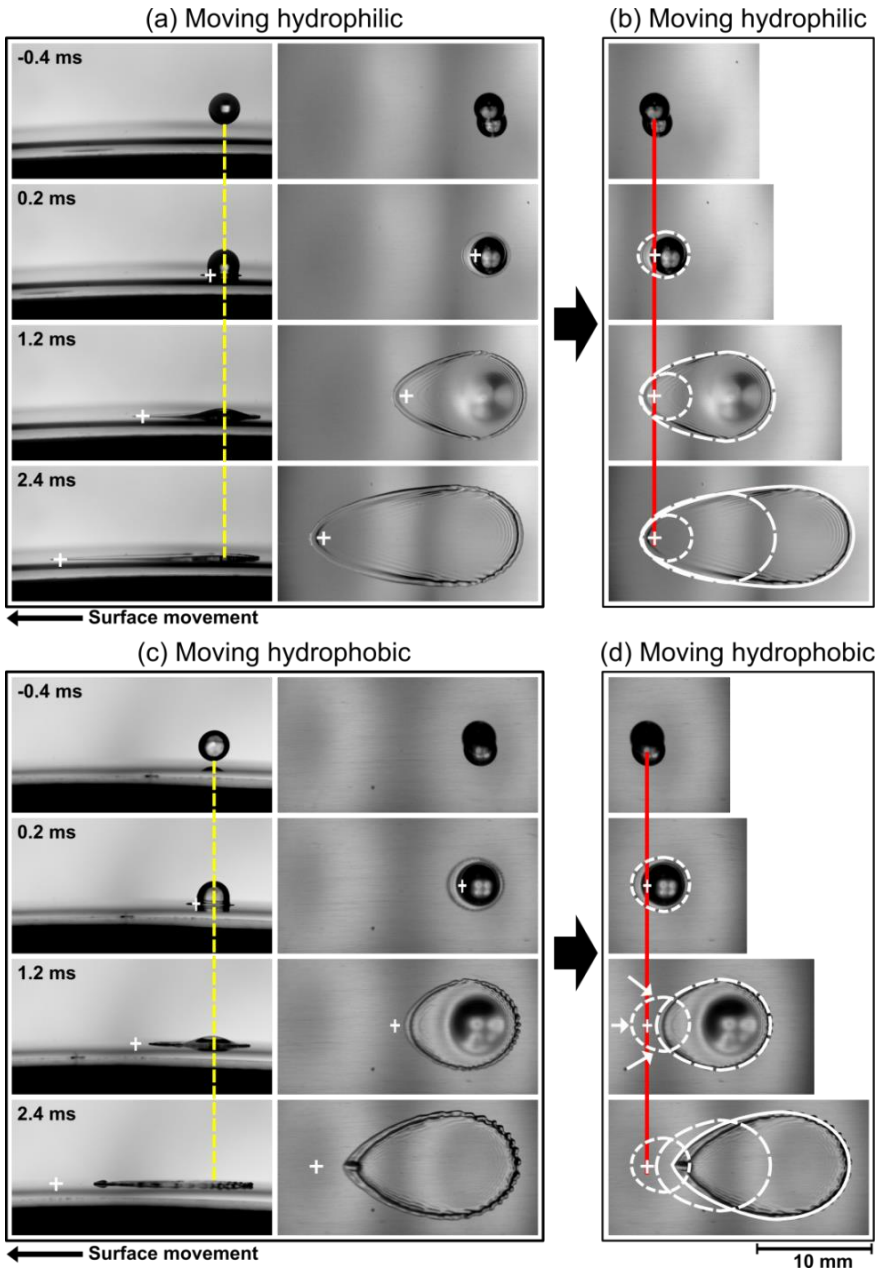

Figure 2.4: Side and overhead views of the water drop impact onto moving hydrophilic (a and b) and hydrophobic (c and d) surfaces. Drop velocity is V_n=2.01 m/s and surface velocities are (a and b) V_s= 5.75 m/s, and (c and d) V_s= 5.65 m/s. Vertical dashed line shows the local for the drop apex; apex only moves in the vertical direction. White cross refers to the drop impact point on a surface where it moves with Vs, i.e. moving away from dashed line (drop apex). Surface moves from right to left. Taking drop impact point as the reference, (b) and (d) show the shifted images of (a) and (c), respectively. Vertical solid line shows the drop impact points. Arrows refer to the lamella movement direction.

Hydrophilic surfaces: Figure 2.4a demonstrates the process of the drop impact onto a moving hydrophilic surface. Upon the drop impact, first the lamella expands in all directions at a very initial time, i.e. t<0.2 ms (the presence of the liquid downstream of the drop impact point confirms this). Lamella expanding in all directions at very initial time (even at direction of surface motion) can be understood by the dominance of the kinetic energy of the drop compared to the momentum transfer by the surface. Then, the lamella stops expanding at downstream and only being stretched by the surface movement; while it continues to expand at upstream until it reaches the maximum width (see Figure 2.4a).

The question is how the lamella behaves during stretching at downstream i.e. whether it remains stationary relative to the surface or recoils? To answer this question, we look at the lamella contact line behavior relative to the surface. To do this, we took the drop impact point as the reference in Figure 2.4b. Note that to have the drop impact process viewed from drop impact point as the reference (Figure 2.4b), each of the selected snapshots from Figure 2.4a has been shifted in space by the surface velocity times the corresponding time interval. The lamella contact line spreads at initial time in all direction. Then, the downstream contact line remains almost stationary relative to the surface (see superimposed outlines of lamella, in Figure 2.4b rows 3 and 4); this implies that the lamella contact line moves with the surface velocity during the stretching at downstream.

The lamella arrest at the downstream can be understood from the fact that the lamella contact line at downstream moves away (with surface velocity) from the bulk of the drop (see vertical dashed line for liquid body location; in Figure 2.4a). Such movement keeps the downstream lamella contact line far from the bulk of the drop where through flattening it feeds the lamella. However, at upstream, since the lamella is near the bulk of the drop, it keeps expanding.

The lamella arrest onset (at t_{arrest}) at downstream can be the instant where the lamella contact line velocity (originated by the drop kinetic energy) is smaller than the surface velocity. When the lamella velocity is less than the surface velocity, it will remain almost pinned to the surface and move with surface velocity. In the time span of interest ($t \leq t_{max}$) this can be explained by: First, liquid-solid contact line at downstream should spend some time (Δt) to change the contact angle from the value reached at the moment of spreading arrest to the value needed for the contact line to recede (see Antonini et al. [30] for details); second, the receding velocity of the contact line will be low as the receding contact angle ($34 \pm 2^{\circ}$) is small [20]. All together this results in a very small displacement at downstream in the time where the receding can happen (= $t-\Delta t- t_{arrest}$, where $t \leq t_{max}$). It should be noted that for some conditions, Δt can be even higher than t_{max} (see Figure 6 in Ref. [30] for details).

Hydrophobic surfaces: Selected snapshots of drop impacting onto a moving hydrophobic surface are shown in Figure 2.4c. The drop behavior and its spreading are very similar to drop impact onto hydrophilic surfaces for $t<0.2$ ms (see the lamella at the downstream of the drop impact point in 2nd row of Figure 2.4c). However, once the lamella stops expanding, it starts recoiling at the outlines of the lamella downstream (while it is stretching at downstream where it connects to the bulk of the drop). The lamella continues to expand at upstream. The recoiling of the lamella at downstream is seen clearly in Figure 2.4d (Figure 2.4d is shifted images in space from that of Figure 2.4c in a similar fashion explained for Figures 2.4a and 2.4b).

Figures 2.5 shows drop impact onto a moving hydrophobic surface, but at a lower drop velocity compared to Figure 2.4c. It is observed that at a similar surface velocity, lower drop velocity causes a more pronounced recoiling of the lamella at downstream and ultimately a tail-lift-off behavior, i.e. jetting and rebounding (Figure 2.5). This behavior of the lamella can be explained

as follows: The shape of the lamella at downstream for lower drop velocities is much elongated; recoiling of such shape means that lamella meets each other quickly in the width direction. Once recoiling fronts meet at the center line, it results in rebounding of a stretched filament of liquid (jetting). The mechanism of rebound is much like drop rebounding on a stationary surface [40], but in this case since the lamella has an asymmetric outline, one observes such elongated filament (see last row Figure 2.5a).

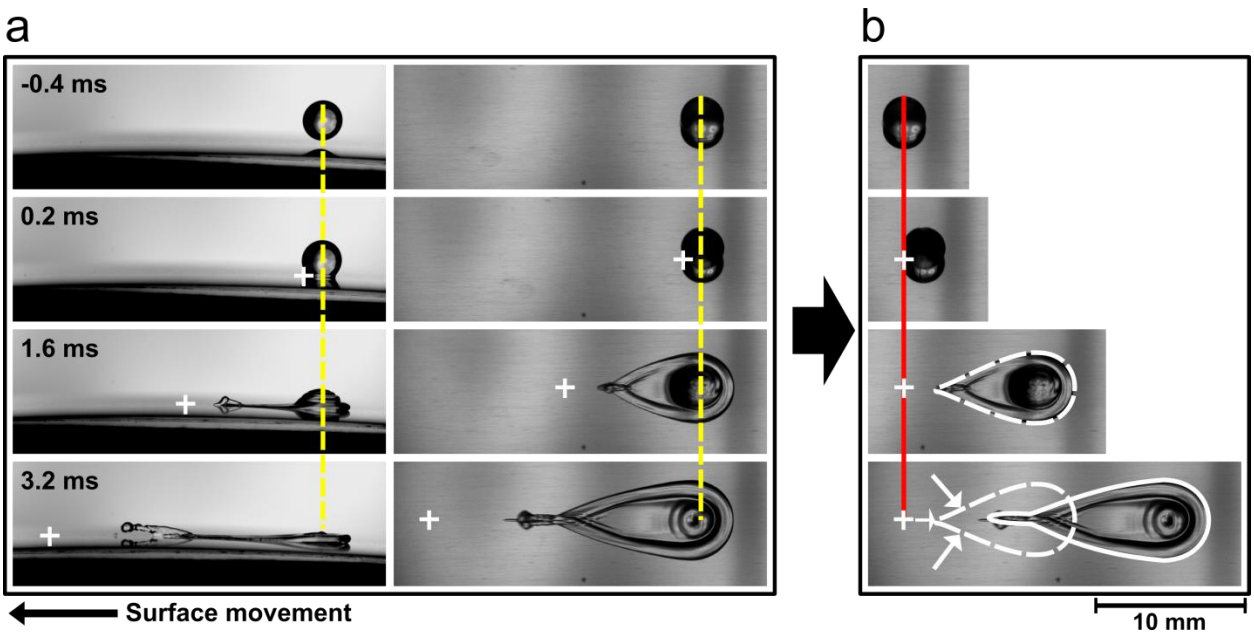

Figure 2.5: Side and overhead views of a water drop impact onto a moving hydrophobic surface. Drop velocity is V_n=0.72 m/s, and surface velocity is V_s= 5.46 m/s. Vertical dashed line shows the local of the drop apex; apex only moves in the vertical direction. White cross refers to the drop impact point on a surface where it moves with V_s, i.e. move away from dashed line (drop apex) with surface velocity. Surface moves from right to left. Taking drop impact point as the reference, (b) shows the shifted images of (a). Vertical solid line shows the drop impact point. Arrows refer to the lamella movement direction.

2.3.1.2 Splashing

Four types of splashing are observed for drop impact onto a moving surface (see Figure 2.6); the convention X-Y is used for naming: X denotes the behavior in the downstream and Y refers to the upstream.

(a) Spreading-prompt splashing (Figure 2.6a): where tiny droplets are generated at upstream contact line of the lamella, while the lamella spreads over the surface at downstream.

(b) Spreading-corona splashing (Figure 2.6b): in this type of splashing some portion of the lamella at upstream lifts off and subsequently detaches, while the lamella is in spreading phase at downstream.

(c) Prompt-corona splashing (Figure 2.6c): this refers to tiny droplets detachment from the advancing contact line at downstream and corona splashing at upstream.

(d) Asymmetric corona splashing (Figure 2.6d): this is lifting off the lamella around the drop contact line in an azimuthally asymmetric form.

Note that the in cases of (a) and (b), spreading behavior of the lamella at downstream is discussed in Section 2.3.1.1.

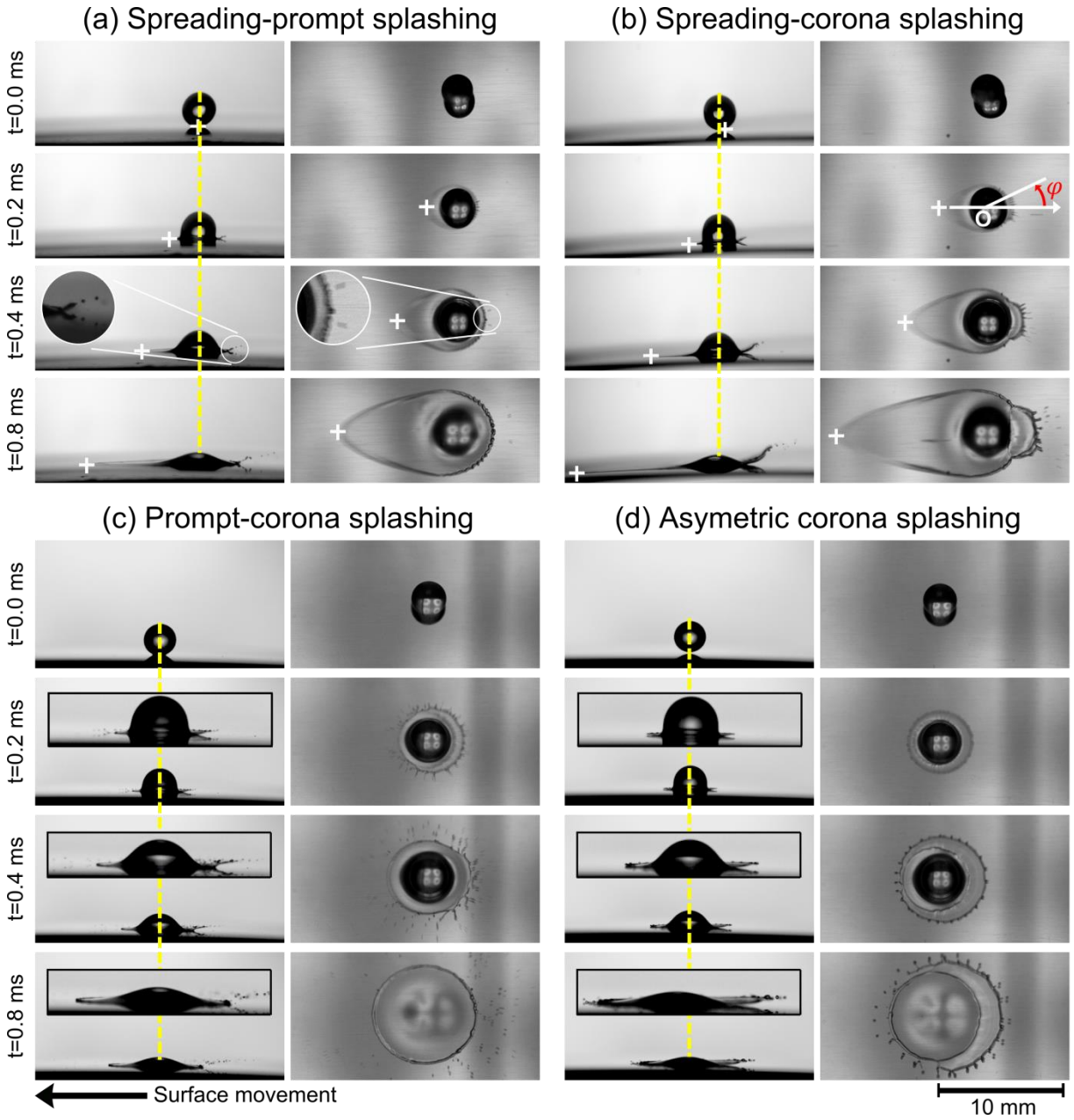

Figure 2.6: Side and overhead views of the drop splashing on a moving hydrophilic surface; zoomed views are provided in the insets. Drop and surface velocities and liquids are: (a) V_n= 2.86 m/s, V_s= 11.5 m/s, and water; (b) V_n= 2.86 m/s, V_s= 14.9 m/s, and water; (c) V_n= 3.2 m/s, V_s= 1.5 m/s, and mixture 1; (d) V_n= 3.2 m/s, V_s= 1.5 m/s, and mixture 2. White cross refers to the drop impact point on a surface where it moves with V_s. Vertical dashed line shows the local of the drop apex. Surface moves from right to left. The φ refers to the splashed portion of the lamella; φ is measured at the instant when the lamella starts to lift off. The azimuthal coordinate (i.e. point o) is centered at the drop apex.

Looking closely, we observe that unlike the understanding in previous studies, the entire lamella in the upstream/downstream does not behave uniformly (Figure 2.6); in fact, the extent of splashing azimuthally differs depending on the drop impact conditions (We_n, Re_n, V_s, and surface wettability). This can be understood by the fact that velocity difference between the surface and liquid film is not uniform over the entire lamella in the upstream/downstream; it gradually decreases in azimuthal direction along the lamella contact line from point $\varphi = 0°$ to $\varphi = 180°$ (see Figure 2.6b). Therefore, considering a 1D model (as done in the literature) will limit the prediction of splashing for only two points (u and d in Figure 2.1b); this does not capture the practical meaning of splashing as one expects. To develop a model for splashing involving a moving surface, unlike the slashing model for stationary surface which can be developed by 1D analysis, a 2D model (lamella azimuthal development) should be considered. The 2D model should be capable of predicting the splashing of the drop as a function of φ (see Figure 2.6b).

2.3.1.2.1 Splashing Model

Here, a model is developed to predict splashing for drop impact onto a moving surface. To do so, the common model for splashing on a stationary surface is considered as the departing point [31,41]:

$$We_n {Re_n}^{\alpha} = K_1 \tag{2.2}$$

where K_1 is a constant which depends on surface roughness. In literature different values are reported for α and K_1 (see Refs [14,31]). In the following we first express the Eq. 2.2 in the form of the velocity differences between the lamella and surface (which is equal to lamella velocity for a stationary surface). Then, the term of the velocity difference will be modified to have a

model which accounts for surface motion as well. To do so, below Eq. 2.2 is expressed as a function of the drop velocity.

$$\frac{\rho^{1+\alpha}D^{1+\alpha}}{\sigma\mu^{\alpha}}(V_n)^{2+\alpha} = K_1 \tag{2.3}$$

Drop velocity can be expressed as a function of the lamella velocity at the time when the splashing initiates based on Rioboux et al. [42] as following:

$$V_n = (2/\sqrt{3})V_l t_l^{\frac{1}{2}} \tag{2.4}$$

where V_l is the lamella velocity at the instance the lamella appears upon drop impact onto a surface; t_l is the instant where the lamella appears. It is understood that the splashing initiates at the instant of lamella appearance [42]. Talking all together, Eq. 2.2 can be rewritten as a function of the lamella velocity as following:

$$\frac{\rho^{1+\alpha}D^{1+\alpha}}{\sigma\mu^{\alpha}}((2/\sqrt{3})V_l t_l^{1/2})^{2+\alpha} = K_1 \tag{2.5}$$

For the drop impact onto a moving surface, the velocity difference between the lamella and surface (the term V_l in Eq. 2.5) is expressed as following (we considered the velocity difference in radial direction, see Figures 2.6b and 2.7b for azimuthal direction, φ):

$$V_{\varphi} = V_l + V_s \cos\varphi \tag{2.6}$$

The value of the φ is to be measured at the instant when the lamella starts to lift off (see Figure 2.6b). Note that the velocity difference between lamella and surface is symmetric with respect to the straight line which passing through *u* and *d* in Figure 2.1b; as a result, the splashing will be symmetric with respect to such line. By applying velocity difference between lamella and surface for moving surface (Eq. 2.6) in Eq. 2.5, one can write:

$$\frac{\rho^{1+\alpha}D^{1+\alpha}}{\sigma\mu^{\alpha}}((2/\sqrt{3})(V_l + V_s\cos\varphi)t_l^{1/2})^{2+\alpha} = K_1 \tag{2.8}$$

The same t_l is assumed for drop impact onto a moving surface as a stationary one [26]. The t_l is expressed as following [42] (for low viscous liquids):

$$t_l = cWe_n^{-2/3} \tag{2.9}$$

where c is a constant. Using the expression for t_l in Eq. 2.8, and rewriting the equation in nondimensional form one has:

$$We_n Re_n^{\alpha} \left(1 + K_2 \frac{V_s}{V_n} We_n^{-1/3} \cos\varphi\right)^{2+\alpha} = K_1 \tag{2.10}$$

Equation 2.10 can be viewed as a general equation to determine the splashing threshold, since by setting V_s to zero, Eq. 2.2 for stationary surface will be recovered.

To determine the values of the α, K_1 and K_2 in Eq. 2.10, 123 experiments with corona splashing were considered for different combination of liquids, surfaces, and drop and surface velocities. We fit the data to Eq. 2.10 using the toolbox cftool in MATLAB. The values of α and K_1 are determined to be $\alpha = -1.0$ and K_1=0.14 for both hydrophilic and hydrophobic surfaces. And, the value K_2 is found to be 4.53 for the hydrophilic surface, and 6.59 for the hydrophobic surface (see Appendix A for curve fitting details).

Figure 2.7a presents the outcomes of the drop impact onto moving hydrophilic and hydrophobic surfaces. Note that the x axis for $\varphi = 180$ is reported as absolute value ($\left|K_2 \frac{V_t}{V_n} We_n^{-1/3} \cos(180°)\right|$). The solid line in Figure 2.7a is the boundary between spreading and when small droplet detachments start to appear (note we deliberately do not use the term splashing as at the threshold only small portion of the lamella exhibits droplet detachments). Although corona splashing data was used to find the constants in Eq. 2.10, it can be seen from Figure 2.7a that practically the solid line is a general boundary; this is so as data points for when

behaviors such as spreading-prompt splashing, and prompt-corona splashing start to appear are also lie near this line.

The band delimited with dashed lines in Figure 2.7a show how Eq. 2.10 also nicely represents the data for cases where splashing takes place over a significant portion of the lamella (note that for $70° < \varphi < 80°$, we use the term splashing since a significant portion of lamella experiences lifting off). The same is true for the interval of $100^{\circ}<\varphi<110^{\circ}$. For graphical clarity we have not shown similar agreements seen for other systems. Note that as x axis in Figure 2.7 is normalized for K_2 values, the plot is useful for both hydrophilic and hydrophobic surfaces.

Figure 2.7b shows the model prediction for drop splashing along the lamella contact line for various conditions of drop impact. It can be seen that the spread of splashing in the azimuthal direction is nonlinear. Splashing from a single point (at $\varphi=0^{\circ}$, i.e. point u as used in 1D models) spreads to say $\varphi=30$ with small changes in V_s or V_n. But splashing a large portion of lamella (say $\varphi>60^{\circ}$) needs a considerably larger change in drop impact conditions. Finally, if drop is splashing in φ direction to a large extent, say if φ is larger than 150°, then small changes in the impact conditions causes the splashing from the entire lamella (similar to impact on a stationary surface where either there is no splashing or entire lamella is splashing, see the cusp in Figure 2.7a or 2.7b)

The experimental results of the Aboud et al. [32] for drop impact onto a moving surface (smooth aluminum) shows good agreement as well (see Figure 2.7b). Note that we used the results of smooth aluminum from Aboud et al. [32] work (see Figure 4b in Ref. [32]) as it has very close wettability to hydrophilic surface used in this study (i.e. K_2 can be considered as 4.53 for their data).

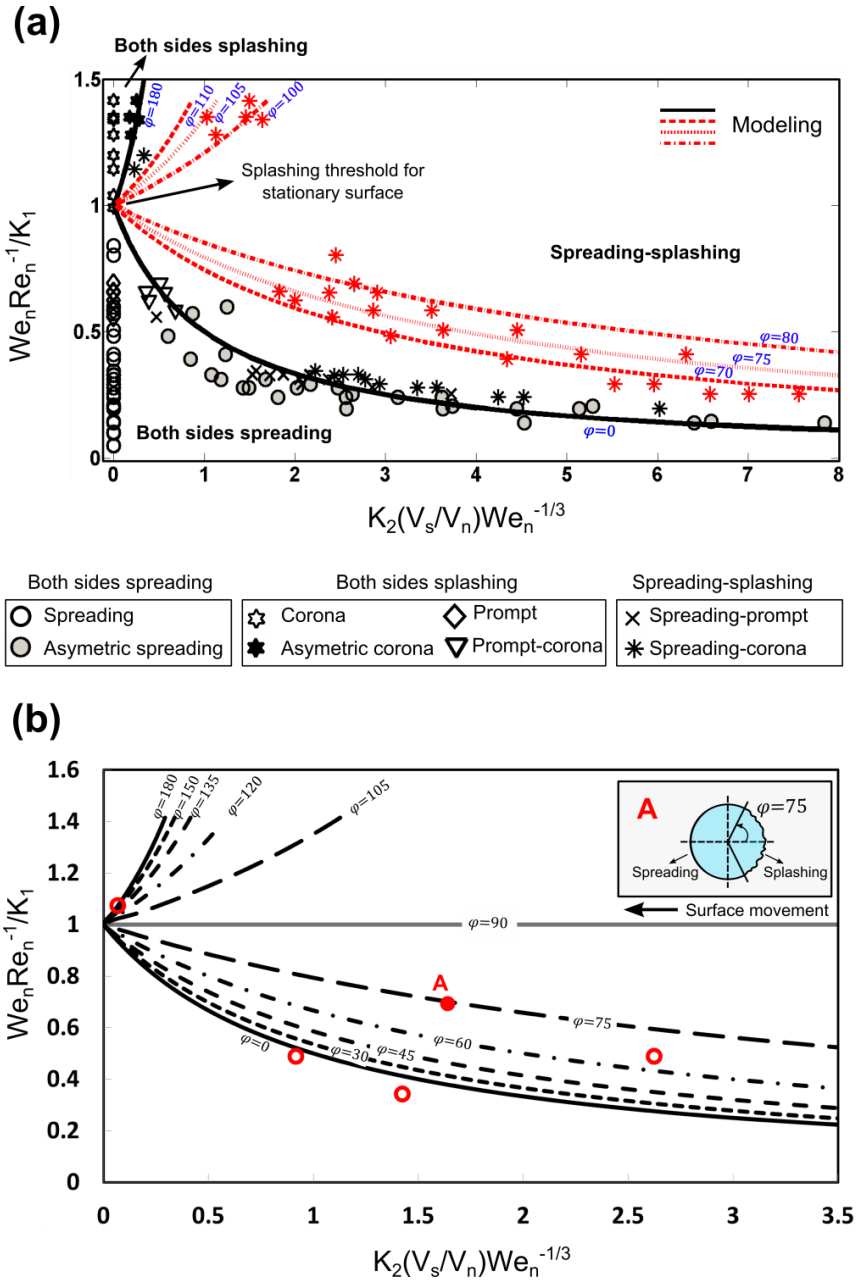

Figure 2.7: (a) Outcomes of water, mixture 1, and mixture 2 drop impact onto moving hydrophilic and hydrophobic surfaces (symbols). Axes are non-dimensionalized considering the parameters in Eq. 2.10. The model predications for $\varphi = 0°$ and $= 180°$ are included. Within the spreading-splashing regime, the splashing happens with different φ values. The experimental data and model predication for φ in the bands of $\varphi = 75 \pm 5°$ and $= 115 \pm 5°$ are provided. (b) Model prediction for the extent of splashing in φ direction (see point A and inset) for various conditions of drop impact onto moving surface is shown. Open symbols show the Aboud et al. [32] experimental data.

Effect of surface velocity: The behavior for the portion of the lamella at the boundary between upstream and downstream (i.e. $\varphi = 90°$) is not affected by surface movement (see the line marked with $\varphi = 90°$ in Figure 2.7b which is independent of surface velocity). If drop impact conditions are such that drop would spreads on a stationary surface (see $We_n {Re_n}^{-1}/K_1 < 1$ regime in Figure 2.7b), the splashed portion of the lamella (φ) increases as the surface velocity increases. However, in the case where drop splashes at stationary surface (see $We_n {Re_n}^{-1}/K_1 > 1$ regime in Figure 2.7b), moving the surface leads to spreading of a larger portion of the lamella ($180° - \varphi$) at the downstream.

Effect of viscosity: The effect of liquid viscosity on splashing of drop impact onto a moving surface has not been studied experimentally to date. We found that at the same drop velocity, an increase of viscosity promotes the splashing (see the value of α in Eq. 2.10). In other words, the spreading possibility becomes limited for higher viscous liquids compared to water. The possible explanation for decreasing of the splashing threshold (for low viscous liquids) can be the higher lamella thickness, as discussed by Ruiter et al. [43]. The higher thickness experiences more lift force by the surrounding air on the edge of the lamella which is one of the main reasons for occurrence of splashing [42].

It should be noted that prediction from the model in Ref. [26] (i.e. Eq. 2.1) indicates a behavior opposite to ours (see power of α); but reliability if the value of α may be in question as in Ref. [26] only one liquid was used. Furthermore, looking at the literature from stationary surface (e.g. Refs. [16,18,19]), one finds that for low viscous liquids (types in this study and Ref. [26]) an increase of viscosity promotes splashing.

Wettability effect: Considering that the values of K_2 is higher for the hydrophobic surface (K_2=6.59) compared to the hydrophilic one (K_2=4.53), it is understood that using a hydrophobic

surface, the lamella splashes with higher φ values compared to the hydrophilic surface. The reason is dewetting of the lamella, which plays a main role in lifting of the lamella, that is easier for hydrophobic surface due to the higher contact angles [20,42]. As such, for a hydrophobic surface the splashed portion of the lamella (highlighted with φ), can stretch the adjunct points ($\varphi + \Delta\varphi$) which are in spreading phase, and subsequently lift to instigate splashing.

2.3.2 Lamella development after t_{max}

Here we present the possible behaviors for drop impact onto a moving surface after the lamella reaches the maximum width.

Hydrophilic surface: For a hydrophilic surface, we observed three different behaviors: recoiling (Figure 2.8a), fingering (Figure 2.8b), and splashing at upstream. In the case of the recoiling, the lamella, due to surface tension, starts to contract towards the center line and finally forms a narrow liquid strip (Figure 2.8a). As it is shown in Figure 2.8a and 2.8b, the increase of the drop velocity, at the same surface velocity (V_s=5.9 m/s), from V_n=1.43 m/s to V_n =3.2 m/s changes the upstream behavior from recoiling to fingering. The undulations in the advancing contact line of the lamella (fingering) are explained using Rayleigh–Taylor instability for an advancing contact line and details can be found in Refs [44,45].

The outcomes of the water drop impact onto a moving hydrophilic surface at $t>t_{amx}$ for a wide range of normal and tangential Weber numbers are presented in Figure 2.9a. Note that in this figure, the symbols show the outcome at $t\leq t_{max}$ (see Section 2.3.1), and the background color highlights the behavior of the lamella at $t>t_{amx}$. For example, for water drop impact at We_n=400 and We_t=4,000, the initial behavior is spreading-prompt splashing, and later outcome is fingering at upstream. When drop experiences corona splashing at $t\leq t_{max}$ at upstream (highlighted with $*$ in

Figures 2.7 and 2.9) the same behavior is seen after t_{max} (highlighted with orange background in Figure 2.9).

The outcomes for mixtures 1 and 2 are presented in Figures 2.9b and 2.9c. For very limited conditions the recoiling is also observed for higher viscous liquids. Fingering behavior was not seen for viscous liquids. Essentially an increase of the viscosity makes the viscous forces dominant over inertial forces and as a result fingering is suppressed [46].

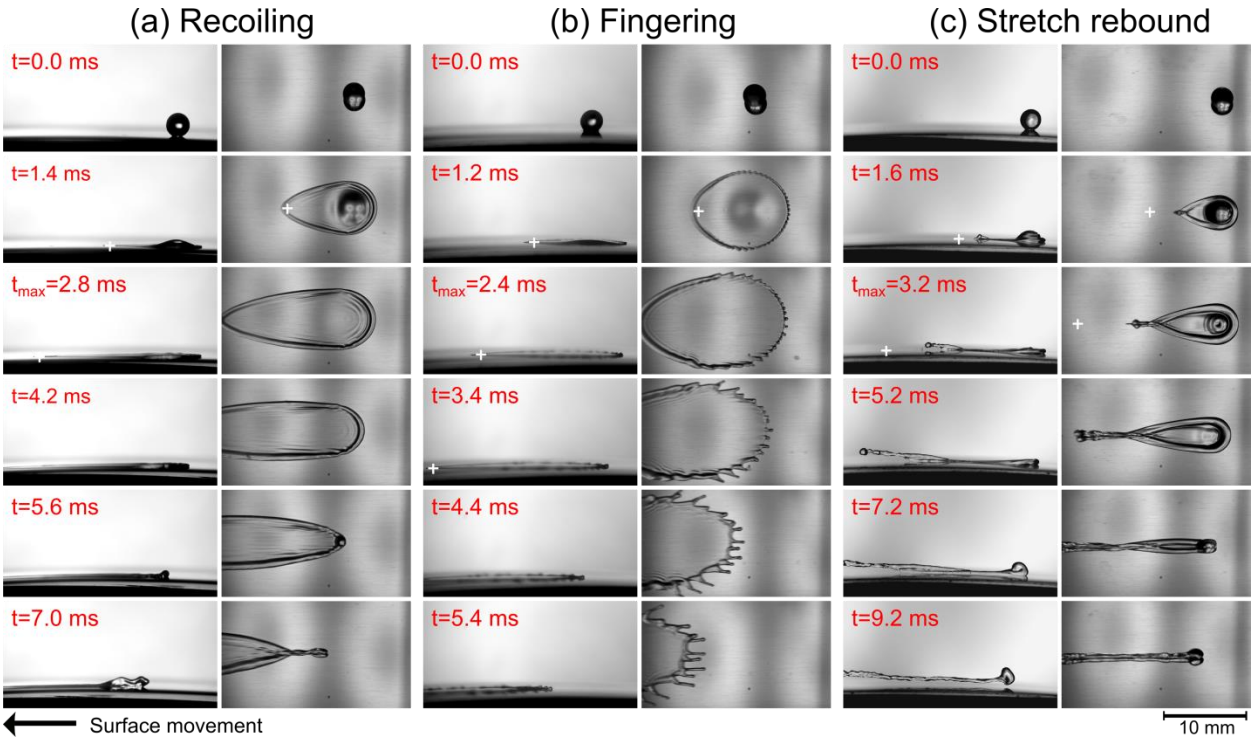

Figure 2.8: Side and overhead views of water drop impact onto moving (a and b) hydrophilic, and (c) hydrophobic surfaces. Drop and surface velocities are (a) V_n=1.4 m/s, V_s=5.9 m/s, (b) V_n=3.2 m/s, V_s=5.9 m/s, and (c) V_n=0.7 m/s, V_s=5.5 m/s.

Hydrophobic surfaces: The lamella on a hydrophobic surface shows the following outcomes at $t>t_{amx}$: fingering, stretch rebound (Figure 2.8c), and splashing. Fingering behavior is discussed in previous section. In the case of the stretch rebound, all of the liquid film over the surface

rebounds from the surface in the form of a narrow liquid filament (Figure 2.8c). Stretch rebound happens following the tail-lift-off mechanism discussed in Section 2.3.1.1 (asymmetric recoil). The lamella lift off starts at the tail part at $t \leq t_{max}$ and extends to whole of the lamella over the surface at $t > t_{max}$, which finally results in rebounding.

The regime maps for various liquids impact onto a hydrophobic surface at $t > t_{amx}$ is presented in Figures 2.9d to 2.9f. For water drop impact (Figure 2.9d), upon drop impact onto a stationary surface, we observed complete rebound for the range of the normal Weber numbers (We_n=17 to 400) studied in this work. Using moving surface, for low tangential Weber number as well as low normal Weber number, the stretch rebound is observed. At the same tangential Weber number, but high normal Weber number, the fingering occurs. For viscous liquids (i.e. mixtures 1 and 2), similar to hydrophilic surfaces, fingering was not observed. Furthermore, the rebounding on a moving surface was suppressed. This can be understood by the fact that, for viscous liquids drop impact, the energy dissipation (i.e. viscous dissipation) is higher during recoiling [40].

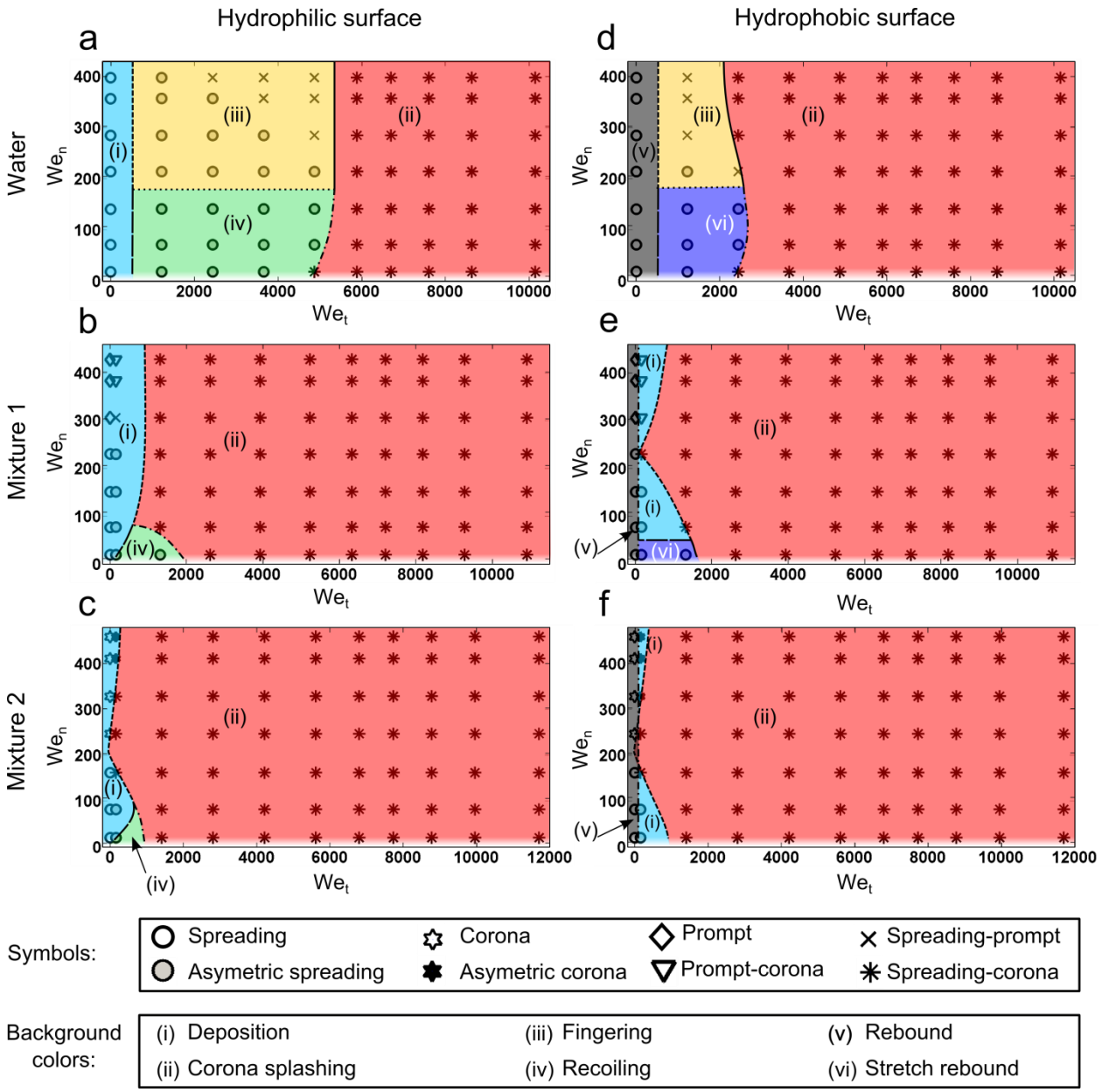

Figure 2.9: Regime maps of the drop impact onto a moving hydrophilic (a-c) and hydrophobic (d-f) surfaces. The liquids are: (a and d) water; (b and e) mixture 1; (c and f) mixture 2. Symbols show the drop impact outcome at $t \leq t_{max}$; background colors refer to the drop impact outcome at $t > t_{max}$. Lines are to guide the eye.

Chapter Three

Asymmetric spreading of a drop upon impact onto a surface: Doppler Effect analogy[2]

3.1 Introduction

Understanding the spreading of a liquid drop on a surface, i.e. the amount and way of wetting of the surface by drop impact, is of fundamental importance for natural and industrial processes [2–6,9]. Many studies are conducted to understand the most simple and basic format of drop impact, i.e. drop spreading over a stationary surface [12–15,47]. Recently, drop impact for complex drop/surfaces are studied to gain practical insights or achieve desired results like reducing the drop interaction time with surface, or controlling the drop deposition [5,24,48–52]. However, drop spreading on a moving surface as one of the most common and practical configuration is rarely studied. Drop spreading over moving surface can be seen in many agricultural and industrial instances including printing (e.g. inkjet printing [2,3]), and spraying (e.g. pesticide [4,5], turbine blades [8,9], and rail industry [6]). Studying the surface motion (i.e. tangential velocity) effect is also helpful in understanding the systems like drop impact onto an inclined surface or drop arriving at an angle onto a surface [26]. Thus, even wider range of

[2] This chapter is to be submitted for publication soon. Authors: Hamed Almohammadi and Alidad Amirfazli

applications can be listed. Here, we experimentally and through modeling investigate the effect of tangential velocity on spreading of drop upon impact onto a surface.

When drop impacts onto a stationary surface (Figure 3.1a), due to high kinetic energy of the drop, it flattens symmetrically as a radially expanding liquid film. This process (called spreading) ends with dissipation of the drop kinetic energy by the surface and viscous forces. The spreading ends when maximum spreading diameter is reached at a certain time, t_{max} (Figure 3.1a). The maximum spreading diameter is expressed as maximum spread factor: $\xi_{max}=D_{max}/D_0$, ratio of the maximum spreading diameter, D_{max}, to the initial drop diameter, D_0. In the literature, many studies have been developed to predict ξ_{max}. The ξ_{max} is found to be dependent on non-dimensional numbers including: the normal Reynolds number ($Re_n=\rho V_n D_0/\mu$, ratio of viscous to the inertia forces, where ρ is the liquid density, V_n is the drop normal velocity, and μ is the liquid dynamic viscosity), and the normal Weber number ($We_n=\rho V_n^2 D_0/\sigma$, ratio of inertia to surface forces, where σ is the liquid surface tension), and surface wettability [30,40,53–59]. In addition, a few studies have been done analytically to predict the time evaluation of spread factor $\xi(t)$ ($=D(t)/D$) for drop impact onto a stationary surface [60–63].

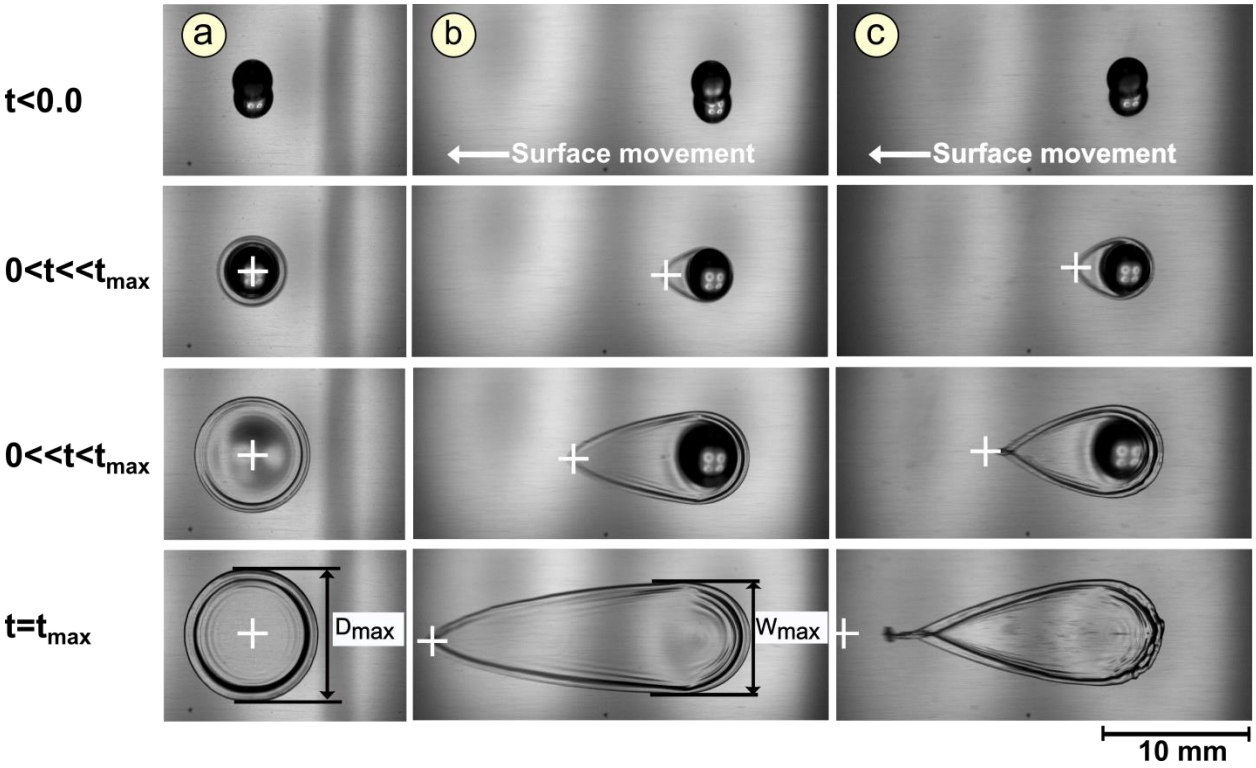

Figure 3.1: Overhead views of the water drop spreading over (a) stationary, and moving (b) hydrophilic and (c) hydrophobic surfaces. Drop velocity is V_n=1.43 m/s and surface velocities are (a) V_t= 0 m/s, (b) V_t= 8.0 m/s, and (b) V_t= 8.0 m/s. White cross denotes the drop impact point on the surface. Surface moves from right to left.

There are relations to describe spreading for a symmetric lamella (i.e. drop spreading on a stationary surface). Previously, we found that when a drop impacts onto a moving surface, it spreads asymmetrically (i.e. has an elongated outline in the direction of surface movement; see Figures 3.1). This is also seen in the literature for drop impact onto inclined surface and other similar systems [32–36], but there is no relation to describe or explain such asymmetric spreading. Note that there are some conditions where drop splashes upon impact onto a moving surface; but we are not concern with these conditions in this chapter. Spreading phase for the drop impact onto a moving surface is defined, as the period from impact until reaching the maximum width for the lamella (W_{max}, see Figure 3.1). The corresponding time to maximum

width is defined as the t_{max}. There are works in the literature and Chapter 2 of this thesis that provides some qualitative initial ideas about spreading, but a comprehensive understanding of how drop and surface velocities affect the lamella shape (both qualitatively and quantitatively) is missing. And, how surface wettability and liquid viscosity change the lamella outline. Put together, the question of how outline of the spreading liquid film evolve overtime for systems with tangential velocity for a drop in not known. The answers to these questions are the basic information to comprehensively understand how tangential velocity affects the spreading of the drop upon impact onto a surface.

To answer the above questions, which comprehensively addresses objective 3 (stated in Chapter 1), here we provide novel hypotheses for the drop spreading behavior over moving surface through an analogy with the Doppler Effect. Using the hypotheses, the effect of the normal and tangential velocities and surface wettability will be discussed. The experimental observation will be reported to verify our hypotheses. Finally, based on developed hypotheses, a model will be developed to mathematically predict not only the maximum spreading of lamella, but also the time evolution of the lamella. The model prediction is validated with the experimental data.

3.2 Methods

Surfaces: Two different surfaces (hydrophilic and hydrophobic) were used in the experiments. A stainless steel surface with advancing and receding contact angles of 89±1˚ and 34±2˚, respectively, was considered as a hydrophilic surface. To fabricate a hydrophobic surface, a solution of FC-75 and Teflon (5:1 (v/v) FC-75, 3-M/Teflon AF, Dupont) was spray coated over the cleaned (with DI water and acetone) stainless steel; where the advancing and receding contact angles were measured to be 123±1˚and 109±1˚, respectively.

Liquids: The glycerol/water mixtures with 0, 24, and 42 % glycerol (w/w) and the viscosities of 1.0, 2.0, and 4.1 mPa.s, respectively, were used as the working fluids [38,39]. The viscosity of the liquids is considered in the range of $\mu/\rho \lesssim 4$ cSt which is referred to as a low viscous liquid in the context of drop impact literature [16–18]. The surface tension and density of the liquids are considered approximately the same, as for the highest concentration of glycerol, the surface tension is decreased from 71.7 to 69.2 mN/m and density is increased from 998.2 to 1104.7 kg/m^3 [38,39].

Impact experiments: All of the experiments were performed at room temperature (20˚C). The experimental setup for the drop impact onto a moving surface is shown in Figure 3.2. Drops with diameter of D_0=2.5±0.1 mm were generated from syringe-needle system. Wide range of normal drop velocities from 0.5 to 3.4 m/s was studied. The tested surfaces were mounted on a rotating large wheel with diameter of D=56.9 cm (see Figure 3.2). Linear velocities in the range of 0 to 17 m/s were generated by rotating the wheel at various rotational velocities. The rotational velocity of wheel was varied by changing the input voltage of a connected motor. The deviation of the surface from horizon in the frame of study is found to be 0.53%, which confirms that one can consider the target surface as flat one. The experiments were recorded by high speed phantom cameras from both side and overhead, respectively, at frame rate of 5,000 and 10,000 fps.

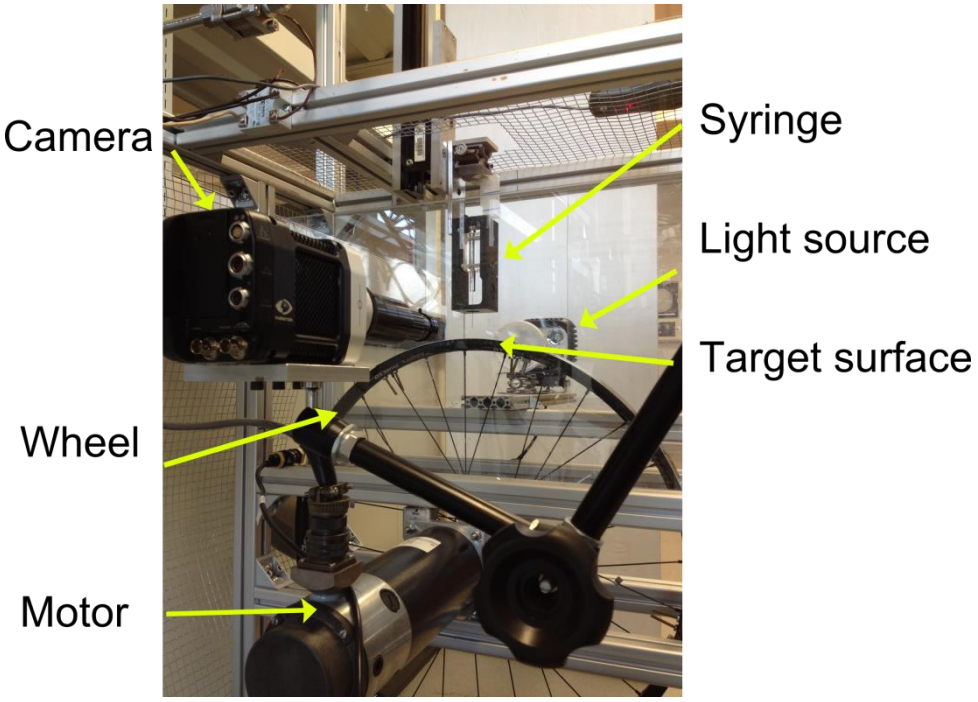

Figure 3.2: Experimental setup for drop impact onto a moving surface

3.3 Results

Drop spreading: Figure 3.2a to 3.2c shows the relative motion of the lamella with respect to the surface for spreading of a drop over stationary and moving surfaces. Drop impact point on a surface is considered as the reference point to observe the lamella behavior. Figures 3.2a to 3.2c show the results in Figures 3.1a to 3.1c, respectively, but with reference to drop impact point.

In the case of drop impact onto a stationary surface (Figure 3.2a), drop spreads radially outwards until it reaches the maximum diameter. The superposed outlines of the lamella at different times ($0<t<t_{max}$) clearly shows the radially spreading of the drop (see Figure 3.2a). The diameter of the circles is $D(t)$ and drop impact point is at the center of all circles. One can take either drop impact point or drop apex as a representative for the center point of outline of lamella; these two points for the drop impact on a stationary surface are always overlapped (see Chapter 2).

Mathematically, one can write the equation of propagation of the circles for spreading of drops on a stationary surface as following (X-Y coordinate origin is located at drop impact point, see Figure 3.2a):

$$y^2 + x^2 = r(t)^2 \tag{3.1}$$

where r(t) (=*D(t)*/2) is the radius of the circles at time, *t*. The radius of the circles, depending on impact, liquid, and surface parameters, differs and can be calculated through the existing models in the literature [60–63]. However, due to the complexity of the existing correlations, here we provide simple relations to calculate r(t) for both hydrophilic and hydrophobic surfaces as following (see Appendix B for details):

Hydrophilic $$\xi(t)/\xi_{max} = 1 - \exp\left(a\left(t/We_t^{-\frac{1}{4}}\right)^b\right) \tag{3.2}$$

Hydrophobic $$\xi(t)/\xi_{max} = 1 - \exp(ct^d) \tag{3.3}$$

where t(ms) is the given time, and a, b, c, and d are fitting coefficients. The values of the coefficients are found to be $a = -0.535$, $b = 0.850$, $c = -1.352$, and $d = 0.815$. The value of ξ_{max} can be calculated through correlations from literature [30,40,53–59].

Upon drop impact onto a moving hydrophilic surface (Figure 3.2b), drop spreads in all directions at the very initial time ($0<t<<t_{max}$ in Figure 3.2b) of impact (the presence of the lamella at the downstream side of the impact point confirms this issue). Then, the lamella stops spreading in one side of the drop (downstream in Figure 3.2b), while it continuous spreading at the other side (upstream in Figure 3.2b) until the maximum width is reached. Note that the upstream and downstream are defined for a given time; and the line of maximum width at any given time defines the boundary between upstream and downstream along the lamella contact line. Arrest of the lamella at downstream can be seen from superimposed outlines of lamella in Figure 3.2b (see white lines).

Using a surface with a lower wettability (i.e. hydrophobic, see Figure 3.2c), changes the behavior of the lamella. The lamella starts recoiling at downstream (see superimposed outlines of lamella in Figure 3.2c).

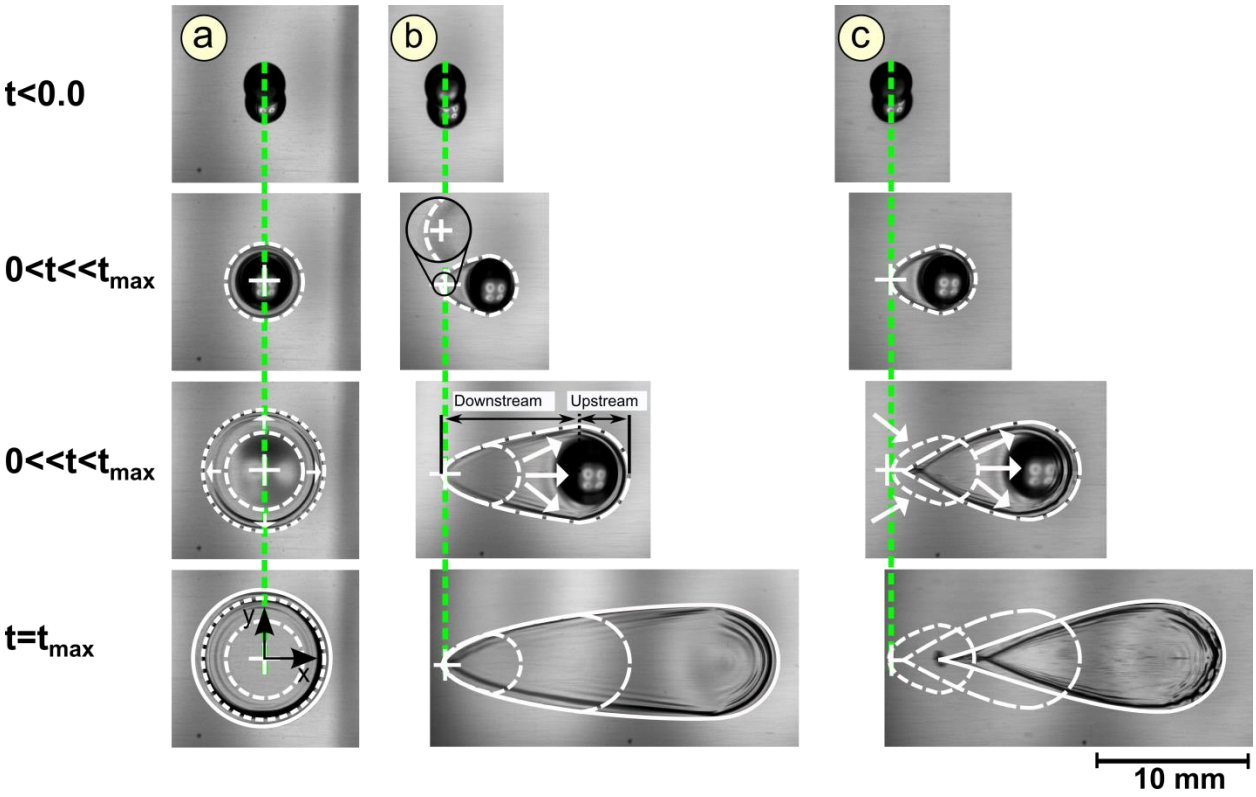

Figure 3.3: Overhead views of a water drop spreading (results from Figure 3.1) with respect to impact point on the surface. Drop impacts on (a) stationary, and moving (b) hydrophilic, and (c) hydrophobic surfaces. Drop velocity is V_n=1.43 m/s and surface velocities are (a) V_t= 0 m/s, (b) V_t= 8.0 m/s, and (c) V_t= 8.0 m/s. White cross denotes to the impact point on a surface, which are aligned along the vertical dashed line. White lines show the superimposed outlines of lamella from consecutive frames shown. Arrows show the lamella motion relative to the surface.

To sum up, in the case of drop spreading on a stationary surface, the lamella outline is symmetric. However, drop spreads asymmetrically over a surface when the surface is moving

(i.e. there is a tangential velocity). The question is can the circles for the drop spreading over stationary surface be used to provide any insights for the outline of a spreading drop over a moving surface? If yes, then how these circles arrange when surface is moving?

Hypothesis development: Doppler Effect describes how the arrangement of wave sound changes from that of radially outward when wave source is moving relative to the medium; then one can think of an analogy between drop lamella outline on a stationary surface and sound source waves in the following way. Based on Doppler Effect, motion of the sound source relative to the medium shifts the center of the each new wavefront with the relative motion velocity. During such process the wavefront magnitude generation is not affected by the movement; in other words, the motion only affects the location of center of each wavefront. As such, two hypotheses can be made to describe how circles can be arranged (lamella outlines for drop spreading on a stationary surface, Figure 3.2a) for when the surface is moving. First, the radius of the circles (r(t) in Eq. 3.1) are not affected by the motion of the surface, i.e. for a given condition and time the radius of each circle is the same for moving and that of a stationary surface (similar to wave propagation). Second, center point of each circle moves with the surface velocity (similar to Doppler Effect). Based on the developed hypotheses, the arrangement of circles in the case of moving the surface is presented in Figure 3.3.

Using the hypotheses, the following will be the equation which predicts how the circles propagate when surface is moving.

$$y^2 + (x - V_s \times \mathrm{t})^2 = r(\mathrm{t})^2 \qquad (3.4)$$

where $V_s \times t$ is the displacement of the circles' center point (which moves with the surface velocity). And, r(t) is the radius of the circles at a given time which is the same as that of the stationary surface (see first hypothesis).

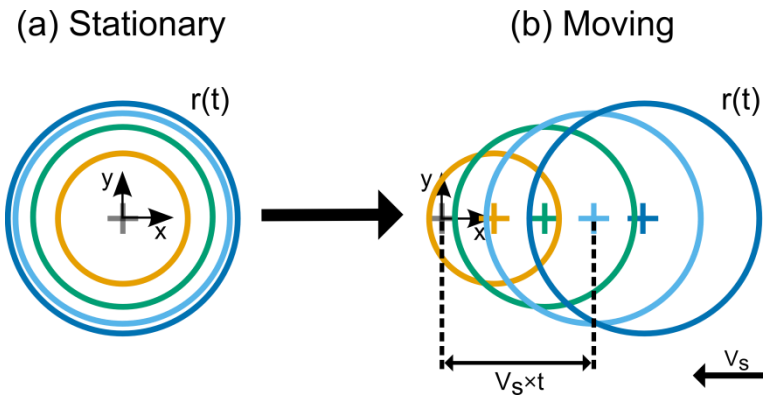

Figure 3.4: (a) Schematic view of the drop lamella outlines on a stationary surface at different times. X-Y coordinate origin is located at the drop impact point, see the grey +. (b) The circle sequence arrangement based on the developed two hypotheses (Eq. 3.4); the circles from (a) are displaced with the surface velocity but keeping the same radius. Colored crosses show the center point of the displaced circles; each pair is highlighted with the same color.

Based on proposed relation for the propagation of the circles (i.e. Eq. 3.2), any changes in drop velocity will result in a change for r(t). As it is understood, increase of the drop impact velocity leads to an increase of the r(t) at a given time [60–63]. As such, Figure 3.4a shows schematically circle sequences for various drop impact velocities (low, medium, and high) at the same surface velocity. Increase of the drop normal velocity results in circles with higher radii, while displacements of the circles are the same at a given time (e.g. consider first circle in each case). Surface motion only affects the displacement of the circles the same as Doppler Effect phenomena for wave front (see Eq. 3.4, where surface velocity changes the $V_s \times t$). Figure 3.4b shows schematically the sequences of circles for various surface velocities at the same normal

drop impact velocity. Increase of surface velocity leads to larger displacement of circles, while the circles' radii are the same at a given time (e.g. consider first or second circle in each case). Taking together, drop normal velocity affects the radius of circles, while any changes in motion of the surface relative to the drop (i.e. tangential velocity) results in changes in distance between centers of two successive circles.

As discussed, during drop spreading over a moving surface the lamella can experience: expansion, pinning, or recoiling (see Figure 3.2). The expansion of the lamella is related to an increase in radius of the circles. For the case of pinning, one can think of circles remaining frozen of the circles after propagation. Following this concept, the recoiling of the lamella can be explained by shrinking of the circles after propagation. As such, Figure 3.4c and 3.4d show schematically sequence of circles representing the outline of a drop spreading over moving hydrophilic and hydrophobic surfaces, respectively. In the case of a hydrophilic surface, the circles remain frozen, while new circles propagate at upstream. For a hydrophobic surface, the circles shrink after propagation stops. Therefore, one can observe smaller circles at downstream for hydrophobic case in comparison to that of hydrophilic one.

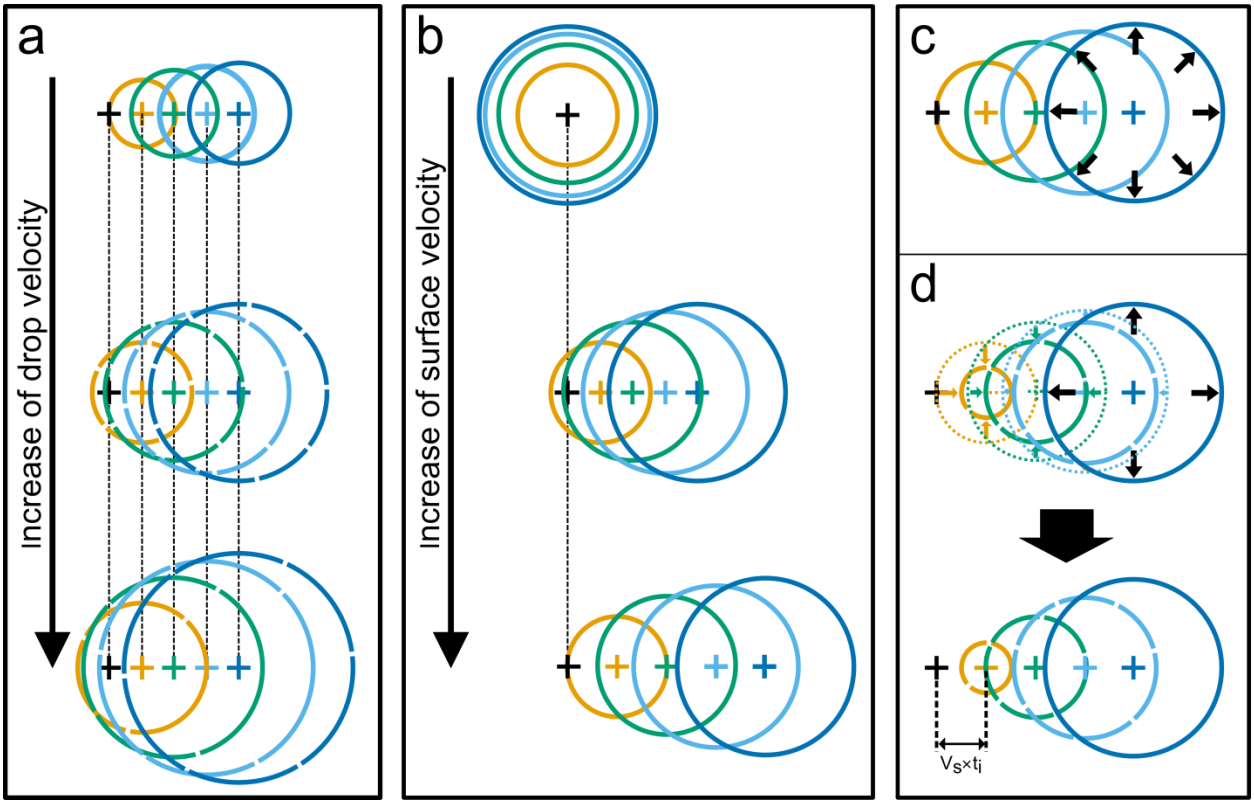

Figure 3.5: Schematic view for (a) drop impact velocity effect, and (b) surface velocity effect on how circles evolve over time. Black cross refers to the drop impact point (as the reference). Colored crosses show the center point of the circles; each pair is highlighted with the same color. (c) Shows schematically the arrangement of the circles over a hydrophilic surface, where the circles remain frozen after propagation. (d) Shows the circle sequence over a hydrophobic surface, the circles experiences recoiling after propagation over a hydrophobic surface.

Hypotheses verification: To evaluate the developed hypotheses, several experiments in wide range of normal drop impact velocities and surface (or tangential) velocities were performed. Drops of liquids with different viscosities and both hydrophilic and hydrophobic surfaces were considered. Starting with the first hypothesis, i.e. the radius of the circles for moving surface (r(t) in Eq. 3.4) is the same as that of stationary one, it was observed that the upstream of the lamella has always a semicircle shape (Figure 3.5a). The radius of the circles of moving case is compared with that of stationary one at a given impact condition in Figure 3.5b. Note that error

bars (representing one standard deviation) are smaller than the symbol sizes in Figure 3.5, which shows high repeatability of data. As it is apparent, at a given time the results are similar for both stationary and moving surfaces. Note that for all of the tested liquids (low viscous liquids), surfaces (both hydrophilic and hydrophobic), and surface velocities, we found the same observation. As such, we can make a conclusion that the first hypothesis is supported by the empirical data.

Next we test whether the circles are moving with the surface velocity or not (second hypothesis). The experimental observations reveal that the apex point (see Figure 3.5a) of the drop always moves with the surface velocity relative to the drop impact point on a surface (see Figure 3.5c and Chapter 2 as well). However, the question is whether the apex is the center of the circle (outline of the lamella) or not? To verify, we consider the center point of the circle with respect to the drop apex (Figure 3.5a). We realized that there is a very small shifting for the center relative to the drop apex point (Figure 3.5a). The possible reason for shifting can be the shear transfer from surface to liquid film. In the end, our second hypothesis is correct by adding a shifting factor as following:

$$X_{disp} = V_s \times \mathrm{t} - C \tag{3.5}$$

where the value of the *C* (shifting factor) depends on drop impact, liquid, and surface parameters. The value of the C is found to be very small and it is provided through empirical correlations in the Appendix B.

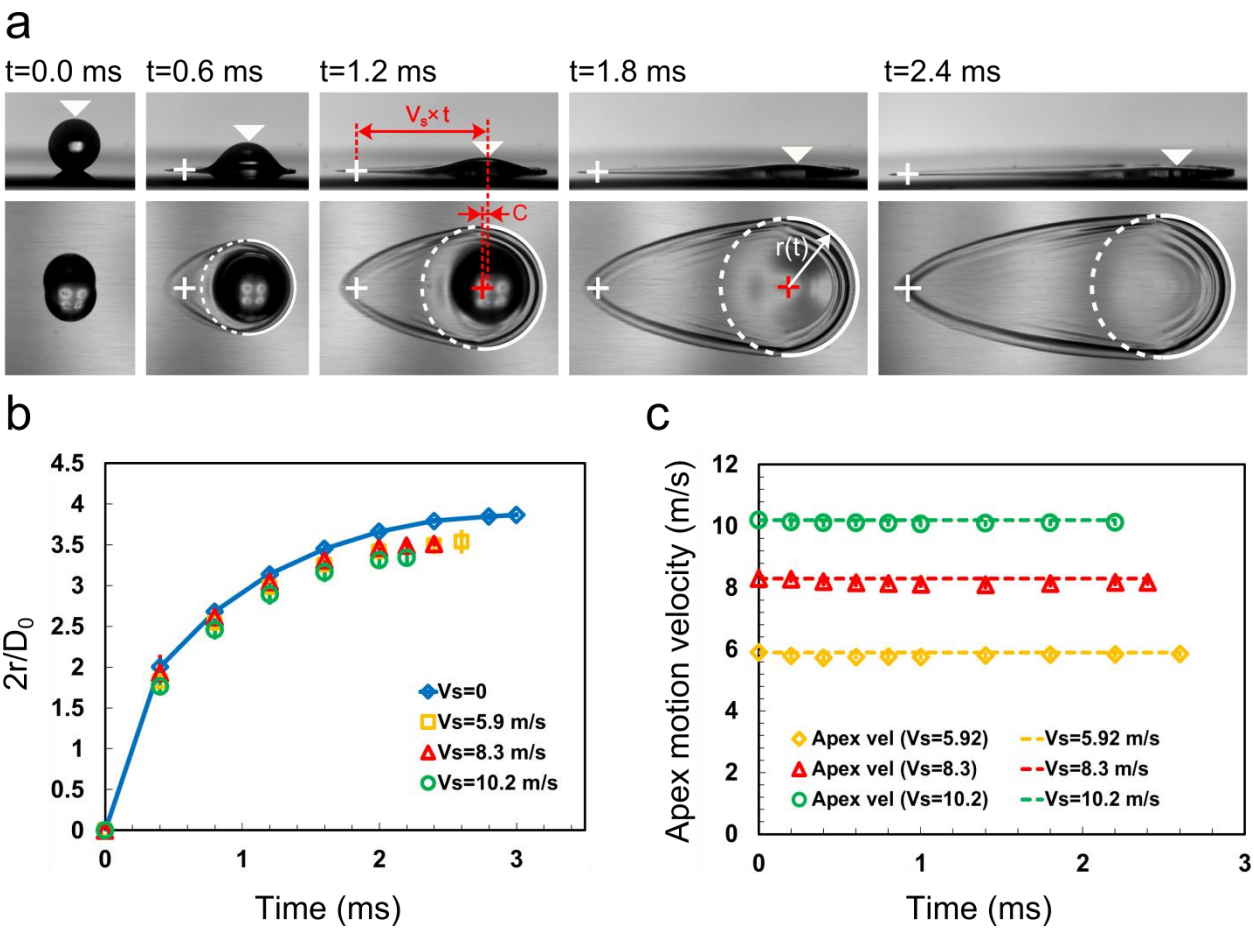

Figure 3.6: (a) Selected snapshots of drop impact (V_n=1.43 m/s) onto a moving surface. White cross refer to the drop impact point on a surface. Red cross shows the circle (lamella outline) center point. Drop apex is denoted with a triangle. (b) Comparison of the lamella circular radius with that of stationary one (V_n=2.01 m/s). (c) The apex location relative to drop impact point for various relative motion velocities; apex moves away from drop impact point with surface velocity (V_n=2.01 m/s).

Model development: Having verified the hypotheses, in following we develop a relation to predict the circle sequence arrangement at a given time considering the circles behaviors after propagation (Figure 3.4c and 3.4d):

$$y^2 + \left(x - X_{disp}(t)\right)^2 = \left(r(t) - V_r(\Delta t)\right)^2 \qquad 0 < t < t_{given} \qquad (3.6)$$

where V_r is the recoiling velocity for the lamella at the downstream and Δt is the time interval which recoiling takes place. Note that $V_r(\Delta t)$ factor indicates that how is the behavior of the circles after propagation; whether the circles remain frozen ($V_r(\Delta t) = 0$) or shrink ($V_r(\Delta t) \neq 0$). The recoil velocity for the liquid film can be expressed as [20]:

$$V_r = \sqrt{2\gamma(1 - \cos\theta_{rec})/\rho h} \tag{3.7}$$

where h is the thickness of the liquid film. The thickness of the lamella can be calculated by having the volume of the liquid film (i.e. how much of the drop is delivered to surface) divided by the area which is covered by the liquid film (see below).

In addition, θ_{rec} is the receding contact angle of the surface. The time which recoiling happens can be calculated as following:

$$\Delta t = \begin{cases} 0 & t_{given} \leq (t + \Delta t_{adv \to rec}) \\ t_{given} - (t + \Delta t_{adv \to rec}) & t_{given} > (t + \Delta t_{adv \to rec}) \end{cases} \tag{3.8}$$

where $\Delta t_{adv \to rec}$ is the residence time that liquid-solid contact line remains pinned as the liquid front stops spreading and starts to recoil. This time increases as the contact angle hysteresis (CAH) increases [30]. Equation 3.8 means that there is recoiling, if $t_{given} > (t + \Delta t_{adv \to rec})$, otherwise there is no recoiling for lamella (Δt will be equal to zero). For the hydrophobic surface studied here, $\Delta t_{adv \to rec}$ is considered to be zero as contact angle hysteresis is small (CAH=14±1˚). For the hydrophilic the recoiling is negligible (i.e. contact line seems pinned, see Figure 3.2b). The reason is explained by high contact hysteresis and low receding angle. The former leads to higher Δt (liquid spends more time to change angle from advancing for spreading to start receding for of recoiling) and the latter leads to a very low recoiling velocity, i.e. $V_r(\Delta t) \approx 0$ (in equation 3.6).

Figure 3.6 schematically shows the sequence of lamella outlines (circles) that are drawn based on Eq. 3.6 for drop impact onto a moving surface. As each circle is a snapshot in time, the outline of the lamella over a moving surface will be the line which envelops all of the circles (i.e. the curve which is tangent to all of the circles).

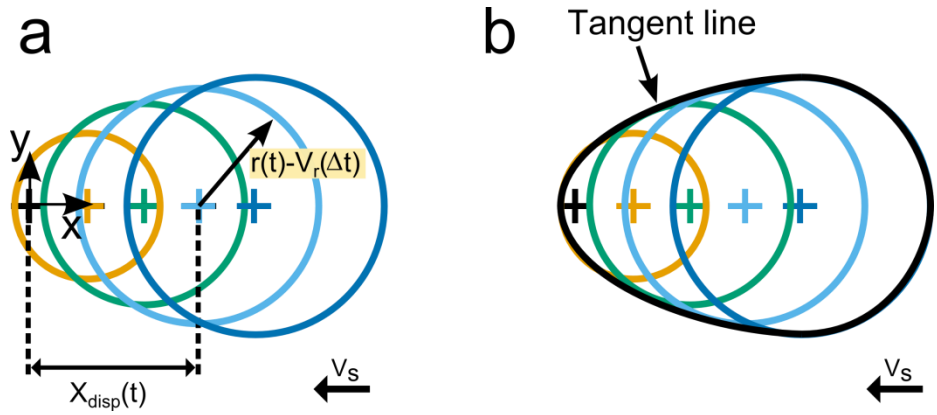

Figure 3.7: (a) Modeling of sequence of circles. Black cross refers to the drop impact point (as a reference). Colored crosses show the center point of the circles; each pair is highlighted with the same color. (b) Tangent line to circles' sequence which envelops all of the circles.

Mathematically, the tangent to circles can be found by solving Eq. 3.6 and its derivative together [64] (see Figure 3.6b):

$$\frac{d}{dt}\left[y^2 + \left(x - X_{disp}(t)\right)^2 = \left(r(t) - V_r(\Delta t)\right)^2\right] \tag{3.9}$$

The resultant solution is noted as: $f_{tangent}(x, y)$.

Having the equation of the line which envelops all of the circles, one can calculate the area which is covered by the liquid film at any given time as following:

$$A = \int f_{tangent}(x, y) \tag{3.10}$$

As such, the thickness of the lamella (assuming being uniform) can be calculated knowing the area (cf. Eq. 3.10); so to be used for calculation in Eq. 3.7.

Figure 3.7 shows the comparison between the model predictions and our experimental observations for various conditions of drop spreading over a moving surface. As it is seen, our model predicts the outline of the lamella very well.

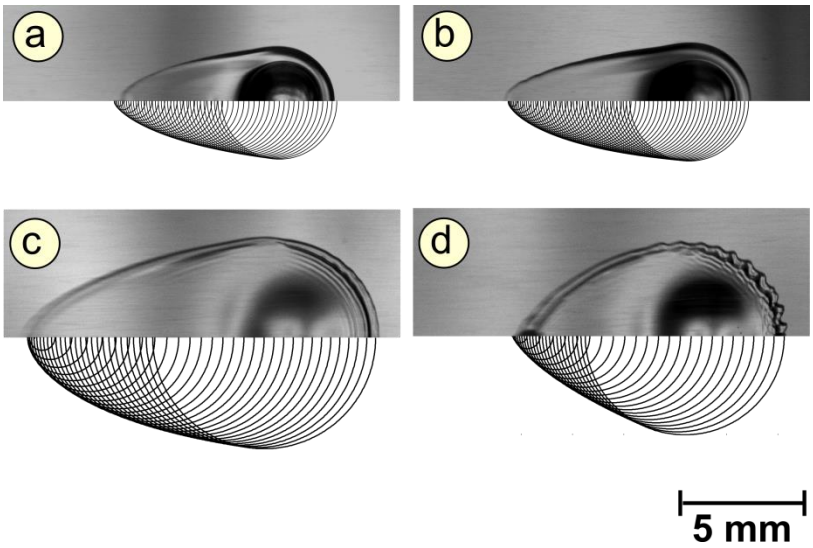

Figure 3.8: Overhead view of drop spreading on a moving (a, b and c) hydrophilic and (d) hydrophobic surfaces. Drop and surface velocities and liquids are: (a) V_n= 0.7 m/s, V_s= 4.17 m/s, and water; (b) V_n= 0.7 m/s, V_s= 3.69 m/s, and mixture 1; (c) V_n= 2.01 m/s, V_s= 8.11 m/s, and water; (d) V_n= 2.01 m/s, V_s= 7.62 m/s, and water. The top of the each panel shows the experimental results and bottom shows to the model prediction (circle series).

3.4 Discussion

It is common for the drop to impact onto a surface in a condition where the impact involves both normal and tangential velocities. Although here we focused on effect of surface motion on drop spreading, the tangential velocity also can be seen in other common systems including drop impact onto an inclined surface or drop arriving at an angle onto a surface. These systems can be seen in many applications from coating and spraying to inti-icing, where it is needed to have controlled wetted area (i.e. minimum, desired, or maximum). Based on the findings in this

Chapter, one is able to design a system with the knowledge of how the tangential velocity affects drop spreading; and as a result, how much area is being wetted by a drop (both qualitatively and quantitatively). For instance, it is revealed that higher normal velocity increases the width of the lamella; and higher surface velocity increases the length of the wetted area. The viscosity plays a role mainly in *r(t)* in equation 3.6. In addition, wettability of the surface changes the area which is wetted by the surface; where there is lower wetted area for hydrophobic surfaces.

Our expectation is that this approach will help to have more understanding of common type of the drop spreading on a surface, as drop does not necessarily impacts perpendicular onto surface in reality. As such, systems with higher efficiency can be designed to get desired results in applications.

Chapter Four

Effect of viscosity on splashing behavior of a drop impacting onto a surface

4.1 Introduction

When drop impacts onto a stationary surface it either spreads or splashes [12–14]. Many studies have been conducted experimentally and numerically to understand when a drop splashes upon normal impact onto a surface; and what is the effect of various parameter on splashing [12–14,16–19]. However, understanding the splashing behavior of the drop upon impact onto a surface still remains one of the challenging areas in the context of the drop impact. Here, the role of viscosity on splashing behavior of a drop upon impact onto a stationary surface will be discussed.

Looking at literature, one can find that governing parameters for drop splashing are as follows: the impact condition (i.e. normal drop velocity, and drop size) [12], liquid (i.e. density, viscosity, and surface tension) [16,17], surface (i.e. roughness), and surrounding medium [19]. The common model which brings the parameters together to predict splashing behavior is defined based on the involving forces (i.e. involves inertia, viscous stress, and surface tension) in splashing, as following [31,41]:

$$We_n Re_n{}^{\alpha} = K \tag{4.1}$$

where K is a constant which depends on surface roughness. As such, most of the studies so far have used this form and found the values of the α and K using best fitted curve to their data. In the literature, different values are reported for α and K (see Table 4.1) [14,31].

Table 4.1: Exiting relations for drop splashing

Source	Value of $\boldsymbol{\alpha}$	Value of $\boldsymbol{K}$	Range of viscosity	Re number range	Increase of Viscosity
Mundo et al. [17]	0.5	115.4	1-3.7	20-2,500	↓
Stow et al. [25]	0.45	f(roughness)	1	3,000-18,000	↓
Bird et al. [26]	0.5	5700	1.2	1,400-5,000	↓
Vander Wal et al. [16]	-0.78	1.7	0.6-4.3	10-15,000	↑
Xu et al. [19]	–	–	0.68-2.6	2,600-35,000	↑
Palacios et al. [41]	–	–	0.65-17	200-20,000	↑↓
Riboux et al. [42]	–	–	0.38-10	–	–,↓*

*this means for low viscous liquids no effect; for high viscous liquid, the splashing chance increases.

However, this model (Eq. 4.1) is defined for normal atmospheric conditions, and does not cover surrounding gas effect. As such, Xu et al. [19] examined surrounding air effect on splashing. They found that reducing the surrounding air pressure suppresses the splashing. They proposed that there are two factors which decide whether drop splashes or spreads: First, the force from the surrounding gas on the lamella which makes the lamella to destabilize (Σ_G); second, surface tension force which keeps the lamella intact (Σ_L). Based on this theory, a new relation for drop splashing is provided as following:

$$\Sigma_G / \Sigma_L = \frac{1}{2} \frac{c_G}{V} \frac{\rho_G}{\rho} WeRe^{-1/2} \tag{4.2}$$

where c_G and ρ_G are, respectively, the speed of the sound and density of the surrounding gas. The drop splashes when ${\Sigma_G}/{\Sigma_L} > 0.45$.

Very recently, Riboux et al. [42] proposed a new theory for splashing which says that to have splashing, two conditions need to be fulfilled simultaneously: First, the liquid of the lamella must dewet the solid surface; and second, the lift force by the surrounding air on the edge of the lamella, which needs to be large enough to avoid the liquid to contact the solid again. As such they developed following model for drop splashing:

$$\begin{cases} \text{High} \quad Oh: & \mu/\mu_G \propto (ReOh_G{}^{8/5})^{-5/4} \\ \text{Low} \quad Oh: & \mu/\mu_G \propto (ReOh_G{}^{8/5})^{-1} \end{cases} \tag{4.3}$$

where $Oh_G = \mu_G/\sqrt{\rho R \sigma}$, and μ_G is the visocity of the surrounding gas. In addition, R is the radius of the impacting droplet.

It is clear that due to the complexity of the phenomena, one can find different theories about the splashing of a drop upon impact onto a surface. Considering of the above models, the main question which arises is what is the role of viscosity on splashing? Some models predict that increase the viscosity promotes the splashing, while others predict the opposite trend (see the trend of the viscosity in Table 4.1).

This issue is acknowledged for the first time by Xu et al. [19], where they observed non-monotonic behavior for pressure threshold (the pressure above which the drop splashes) versus liquid viscosity. As such, they categorized the liquids into two: low viscous liquids ($\mu/\rho \lesssim 4cSt$), and high viscous liquids ($\mu/\rho \gtrsim 4cSt$). For the low viscous liquids, increase in viscosity promotes the splashing; while for high viscous liquids increase in viscosity suppresses the splashing. It is explained that for low viscous liquids increase in viscosity increase the film thickness, which result in splashing. But for high viscous liquids, it is explained that increase in

viscosity helps the liquid film to stabilize the spreading drop. With respect to this explanation, still the reason for such non-monotonic is lacking, as the thickness of the lamella increases with an increase in viscosity for high viscous liquids as well.

Recently, Palacious et al. [41] justified that the reason of the contradiction in literature is because of viscosity range which have been studied by the literature. As such, they provided series of the experiments on wide range of the liquid viscosity. The same observation (i.e. non-monotonic effect of liquid velocity on splashing) is made by Palacios et al. [41]. They defined the *Re*=1,000 for the boundary of such behavior. Above *Re*=1,000, increase of the viscosity changes the spreading to splashing, the same as low viscous liquids. Again, no physical explanation is provided by the authors.

Considering mentioned points to comprehensively address the objective 5 (provided in Chapter 1), two main issues need to be addressed:

- First, what is the sufficient criterion to define the boundary between the low viscous and high viscous liquids in drop splashing context? For example, if one uses liquids in the viscosity range of $\mu/\rho \lesssim 4cSt$ (which is defined as a low viscous liquid by Xu et al.), but at high Reynolds number, i.e. *Re*<1,000 (which is defined as region which show opposite behavior to low viscous liquids), then what will be the trend? As an example, see Mundo et al. [17] and Vander Wal et al. [16] in Table 4.1, which predict opposite behaviors for the same range.

  Therefore, there is a need for a criterion which answers this question. This issue can be addressed by understanding the role of viscosity on splashing.

- Second, as the main scope of this chapter, what is the reason of such non-monotonic behavior? This will help with the understanding of drop splashing phenomena as well as providing more comprehensive theory.

To address these issues, here we will provide experimental study of drop impact onto a surface at the wide range of liquid viscosity. Then, for the first time, the reason of such non-monotonic behavior of the viscosity will be explained in details. Finally, our suggestion for developing a criterion to categorize the liquids will be presented.

4.2 Methods

The experimental setup, used for this study, includes target surface, syringe, high speed camera. The syringe was placed at different heights above the target surface to generate drops with different velocities. A stainless steel surface was considered as a target surface. The target surface has advancing and receding contact angles approximately 89° and 34°, respectively. The high speed Phantom camera was used to record the experiments at at frame rate 10,000 fps.

The glycerol/water mixtures were used as the working fluids. The wide range of liquid viscosity (1-188 cSt) is considered. For the highest concentration of glycerol, the surface tension is decreased from 71.7 to 65.2 mN/m (9%) and density is increased from 998.2 to 1238.1 kg/m^3 (24%) [38,39]; As such, considering the changes in liquid viscosity, the surface tension and density of the liquids are considered approximately the same.

4.3 Results and discussion

Figure 4.1 shows our experimental data of drop impact onto a stationary surface for various liquid viscosities. As it is seen, at the same drop velocity (say V_n=3 m/s), increase in the viscosity (up to $\approx 5\ Sct$) changes the behavior of the drop from spreading to splashing; more increase in viscosity (higher than 5 Sct) results spreading again. This shows the non-monotonic behavior of the drop splashing with changes in liquid viscosity.

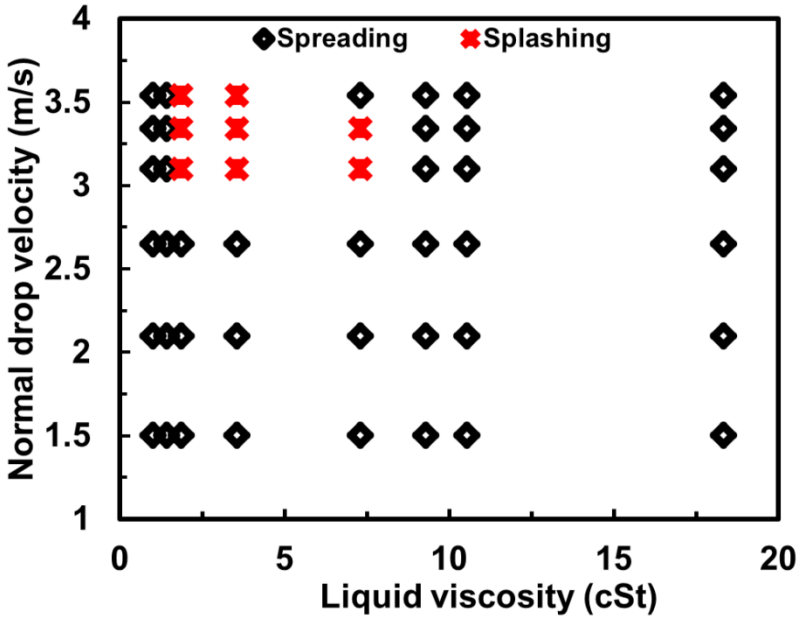

Figure 4.1: Outcomes of drops of liquids with different viscosities impact onto a surface

Why this monotonic behavior is happening? To answer, one needs to understand what will change in drop impact process if one increases the viscosity of the liquid. Figure 4.2 shows the results of drops of liquids with different viscous impact onto a surface at spreading condition. Note that here we look at drop impact process on spreading phase, and we will expand our understanding to splashing. An increase in viscosity has two main effects: (1) the thickness of the lamella increases (see Figure 4.2, where $h_2 > h_1$; this has been confirmed in literature as well), the

higher thickness experiences more lift force by the surrounding air on the edge of the lamella which is one of the main reasons for occurrence of splashing; (2) lamella spreading velocity decreases (see the length of the spreading diameter at a given time for different viscosity in Figure 4.2; for instance at the same given time $D_2<D_1$). As such, the lift force by the surrounding air on the edge of the lamella decreases. All in all, increase of the liquid viscosity, from one side promotes splashing; from other side suppress the splashing. As such, the output depends on whether the promoting or suppressing factor is dominance.

Based on the provided explanation, the determining factor to categorize the liquids should be as a function of the lamella thickness and lamella velocity. This can be done by experimentally measuring the thickness and lamella velocity for different drop velocities as well as liquids with different viscosities.

Note that developing a criterion is not the focus of this chapter. Our main goal was to understand the non-monotonic trend of splashing with an increase in liquid viscosity.

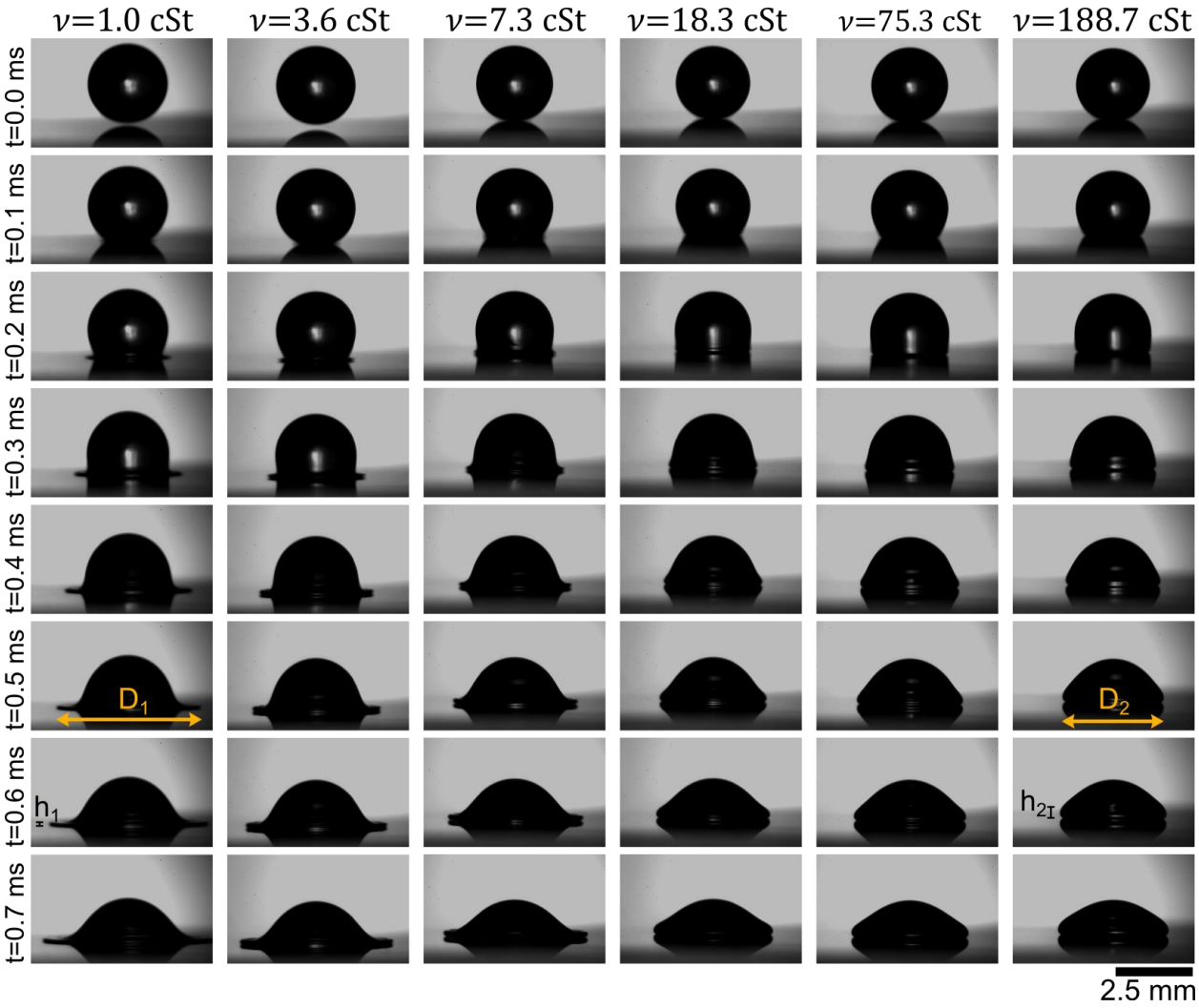

Figure 4.2: Drops (D_0=2.5 mm) of liquids with different viscosities impact onto a surface.

Chapter Five

Conclusion and future Works

Here, the conclusion of the thesis will be provided. In addition, the potential work for the future with the knowledge has got in this thesis will be provided.

5.1 Conclusions

For objectives 1, 2, and 4 (stated in Chapter 1), we performed a systematic experimental study to understand drop impact onto moving hydrophilic and hydrophobic surfaces. Liquids of various viscosities were used. Two main stages of the lamella development are defined for drop impact onto a moving surface: lamella extension stage ($t \leq t_{max}$) and lamella retraction stage ($t > t_{max}$). At lamella extension stage, it was found that drop spreads asymmetrically (i.e. elongated outline) over the moving surface. The mechanism of such asymmetric spreading (i.e. expanding, pinning, and recoiling process) was discussed in details. It was found that wettability of the surface significantly affects the downstream behavior of the lamella. It was also found that drop splashes azimuthally asymmetrically over the moving surface. Splashing probability is the highest at $\varphi = 0°$ and lowest at $= 180°$; and it gradually decreases along the lamella contact line from point with $\varphi = 0°$ to $\varphi = 180°$. A new model was developed to describe such azimuthally asymmetric behavior of the splashing which is a function of We_n, Re_n, V_n, V_s, and of the surface wettability. For hydrophobic surface, a larger portion of the lamella lifts off the surface in comparison to the hydrophilic surfaces. In addition, it was experimentally found that an increase

of liquid viscosity decreases the splashing threshold. Finally, comprehensive regime maps for the outcomes of the drop impacting onto a moving surface were provided for both lamella extension and retraction stages.

For objective 3, we studied how the parameters of drop and surface velocities, surface wettability, and liquid viscosity affect the spreading behavior of a drop upon impact onto a moving surface. A model was developed to mathematically predict not only the maximum spreading of lamella, but also time evolution of the lamella.

Although here we focused on effect of surface motion on drop spreading, the tangential velocity also can be seen in other common systems including drop impact onto an inclined surface or drop arriving at an angle onto a surface. These systems can be seen in many applications from coating and spraying to anti-icing, where it is needed to have controlled wetted area (i.e. minimum, desired, or maximum). Based on the findings in this thesis, one is able to design a system with the knowledge of how the tangential velocity affects drop spreading; and as a result, how much area is being wetted by a drop (both qualitatively and quantitatively). For instance, it is revealed that higher normal velocity increases the width of the lamella; and higher surface velocity increases the length of the wetted area. The viscosity plays a role mainly in r(t) in equation 3.6. In addition, wettability of the surface changes the area which is wetted by the surface; where there is lower wetted area for hydrophobic surfaces.

5.2 Possible future studies

In this thesis, we provide an experimental study of drop impact onto a moving surface. Based the insights gained this study, some further works are raised. These works can help with the further understanding of the drop impact onto a surface.

Studying numerically drop impact onto a moving surface is suggested as a first potential work. This study will help to understand the velocity field inside liquid film of the drop over the surface. As a result, one can understand how the drop feeds the surface while it stays fixed at drop impact point. In addition, to what extent of lamella thickness the surface motion influences the lamella. The shifting factor (discussed in Chapter 4) can be understood. Furthermore, the dewetting process of the lamella at downstream (see Chapter 3 and 4) can be studied in more details. This study can be done using the FLUENT software. The first suggestion for this work will be studying and understanding numerically the system of normal drop impact onto a surface, as there are many complex issues in this work itself. Having validated system (numerical solution) for normal drop impact onto a stationary surface, the system can be modified to drop impact onto a moving surface.

Understanding how a drop impacts onto a moving surface for high viscous liquids is also practically important. For high viscous liquids, the shifting factor (discussed in Chapter 4) will be different from that of low viscous liquids. We believe that the Doppler Effect can again be very helpful in formulating the spreading of high viscous liquids. We think that, for high viscous liquids, the supersonic form of Doppler Effect (where the source is moving in front head of the wave fronts) will be helpful, as it is expected that upon the drop impact onto a moving surface drop will be at upstream point of the lamella for high viscous liquids. In other words, once the liquid is being delivered over the surface, it is being transferred with the surface velocity.

Understanding whether there is difference between the systems of the drop impact on inclined surface and drop impact onto a moving surface can be other potential work. For both systems, the impact involves both normal and tangential velocities. However, in the case of drop impact onto a moving surface, drop has only normal component of the velocity and momentum transfers

from the surface to the liquid in tangential direction. On the other side, for the case of drop impact onto an inclined surface, drop has both normal and tangential component of the velocity. As such, the momentum transfer process is different from that of moving surface. The suggestions for designing of the experimental setup for this purpose are as follow: First, studying drop impact onto a moving surface and drop impact onto an inclined surface at two different systems and compare the results. Second, studying the drop impact onto a moving surface, where the surface is inclined in the perpendicular direction to the surface motion. Having the surface velocity equal to tangential velocity from inclination (which is calculated from inclined surface structure), if the systems of momentum transfer is same, one should expect to have symmetric behavior with respect to the bisector of two tangential direction. This work can really help to link all of the studies from drop impact onto moving surface, to oblique drop impact onto a surface and drop impact onto an inclined surface, and provide a comprehensive study in the area of drop impact. As such, for start one can think of low viscous liquids as working liquids, as most of the studies so far have been done with low viscous liquids.

Studying in more details the effect of liquid viscosity on splashing is one of the important issues in this area. This will provide insights on how drop splashes upon impact onto a surface, as this topic is not understood comprehensively yet. The different sets of the experiments with liquids with the same surface tension and density, but different viscosities are suggested. Wide range of the liquid viscosity can help to ensure all of the possible behaviors are captured. Our other suggestion will be studying not only the splashing behavior, but also spreading behavior of different liquid viscosities. Understanding the spreading can help with how the lamella thickness and lamella spreading velocity change with change in liquid viscosity. This information is of importance in determining drop splashing.

Although here we studied the effect of the wettability, but it is required to conduct a study to understand how surfaces with extreme wettabilities (like superhydrophobic or superhysrophilic surfaces) affect the drop impact behavior on a moving surface. Understanding drop impact behavior over superhydrophobic surfaces can provided helpful information for applications where it is desired to have minimum drop and surface interaction time like in icing [10, 48, 50].

Bibliography

(1) Zable, J. L. Splatter During Ink Jet Printing. *IBM J. Res. Dev.* **1977**, *21*, 315–320.

(2) van Dam, D. B.; Le Clerc, C. Experimental Study of the Impact of an Ink-Jet Printed Droplet on a Solid Substrate. *Phys. Fluids* **2004**, *16*, 3403−3414.

(3) Wijshoff, H. The Dynamics of the Piezo Inkjet Printhead Operation. *Phys. Rep.* **2010**, *491*, 77–177.

(4) Wirth, W.; Storp, S.; Jacobsen, W. Mechanisms Controlling Leaf Retention of Agricultural Spray Solutions. *Pestic. Sci.* **1991**, *33*, 411–420.

(5) Bergeron, V.; Bonn, D.; Martin, J.; Vovelle, L. Controlling Droplet Deposition with Polymer Additives. *Nature* **2000**, *405*, 772–775.

(6) Suda, Y.; Iwasa, T.; Komine, H.; Tomeoka, M.; Nakazawa, H.; Matsumoto, K.; Nakai, T.; Tanimoto, M.; Kishimoto, Y. Development of Onboard Friction Control. *Wear* **2005**, *258*, 1109–1114.

(7) Eadie, D. T.; Santoro, M. Top-of-Rail Friction Control for Curve Noise Mitigation and Corrugation Rate Reduction. *J. Sound Vib*. **2006**, *293*, 747−757.

(8) Li, N.; Zhou, Q.; Chen, X.; Xu, T.; Hui, S.; Zhang, D. Liquid Drop Impact on Solid Surface with Application to Water Drop Erosion on Turbine Blades, Part I: Nonlinear Wave Model and Solution of One-Dimensional Impact. *Int. J. Mech. Sci.* **2008**, *50*, 1526–1542.

(9) Zhou, Q.; Li, N.; Chen, X.; Xu, T.; Hui, S.; Zhang, D. Liquid Drop Impact on Solid Surface with Application to Water Drop Erosion on Turbine Blades, Part II: Axisymmetric Solution and Erosion Analysis. *Int. J. Mech. Sci.* **2008**, *50*, 1543–1558.

(10) Antonini, C.; Innocenti, M.; Horn, T.; Marengo, M.; Amirfazli, A. Understanding the

Effect of Superhydrophobic Coatings on Energy Reduction in Anti-Icing Systems. *Cold Reg. Sci. Technol.* **2011**, *67*, 58–67.

(11) White, E. B.; Schmucker, J. A. A Runback Criterion for Water Drops in a Turbulent Accelerated Boundary Layer. *J. Fluids Eng.* **2008**, *130*, 61302.

(12) Yarin, A. L. Drop Impact Dynamics: Splashing, Spreading, Receding, Bouncing⋯. *Annu. Rev. Fluid Mech.* **2006**, *38*, 159−192.

(13) Josserand, C.; Thoroddsen, S. T. Drop Impact on a Solid Surface. *Annu. Rev. Fluid Mech.* **2015**, *48*, 365−391.

(14) Marengo, M.; Antonini, C.; Roisman, I. V.; Tropea, C. Drop Collisions with Simple and Complex Surfaces. *Curr. Opin. Colloid Interface Sci.* **2011**, *16*, 292−302.

(15) Rioboo, R.; Tropea, C.; Marengo, M. Outcomes from a Drop Impact on Solid Surfaces. *Atomization Sprays* **2001**, *11*, 155−165.

(16) Wal, R. Vander; Berger, G.; Mozes, S. The Splash/non-Splash Boundary upon a Dry Surface and Thin Fluid Film. *Exp. Fluids* **2006**, *40*, 53–59.

(17) Mundo, C.; Sommerfeld, M.; Tropea, C. Droplet-Wall Collisions: Experimental Studies of the Deformation and Breakup Process. *Int. J. Multiphase Flow* **1995**, *21*, 151−173.

(18) Xu, L. Liquid Drop Splashing on Smooth, Rough, and Textured Surfaces. *Phys. Rev. E* **2007**, *75*, 056316.

(19) Xu, L.; Zhang, W.; Nagel, S. Drop Splashing on a Dry Smooth Surface. *Phys. Rev. Lett.* **2005**, *94*, 184505.

(20) Bartolo, D.; Josserand, C.; Bonn, D. Retraction Dynamics of Aqueous Drops Upon Impact on Non-Wetting Surfaces. *J. Fluid Mech.* **2005**, *545*, 329–338.

(21) Latka, A.; Strandburg-Peshkin, A.; Driscoll, M. M.; Stevens, C. S.; Nagel, S. R. Creation

of Prompt and Thin-Sheet Splashing by Varying Surface Roughness or Increasing Air Pressure. *Phys. Rev. Lett*. **2012**, *109*, 054501.

(22) Bayer, I.; Megaridis, C. Contact Angle Dynamics in Droplets Impacting on Flat Surfaces with Different Wetting Characteristics. *J. Fluid Mech.* **2006**, *558*, 415–449.

(23) Antonini, C.; Villa, F.; Bernagozzi, I. Drop Rebound after Impact: The Role of the Receding Contact Angle. *Langmuir* **2013**, *29*, 16045–16050.

(24) Grishaev, V.; Iorio, C. S.; Dubois, F.; Amirfazli, A. Complex Drop Impact Morphology. *Langmuir* **2015**, *31*, 9833–9844.

(25) Stow, C. D.; Hadfield, M. G. An Experimental Investigation of Fluid Flow Resulting from the Impact of a Water Drop with an Unyielding Dry Surface. *Proc. R. Soc. A Math. Phys. Eng. Sci.* **1981**, *373*, 419–441.

(26) Bird, J.; Tsai, S.; Stone, H. Inclined to Splash: Triggering and Inhibiting a Splash with Tangential Velocity. *New J. Phys.* **2009**, *11*, 063017.

(27) Dhiman, R.; Chandra, S. Rupture of Thin Films Formed during Droplet Impact. *Proc. R. Soc. A Math. Phys. Eng. Sci.* **2010**, *466*, 1229–1245.

(28) Renardy, Y.; Popinet, S.; Duchemin, L.; Renardy, M.; Zaleski, S.; Josserand, C.; Drumright-Clarke, M. A.; Richard, D.; Clanet, C.; Quéré, D. Pyramidal and Toroidal Water Drops after Impact on a Solid Surface. *J. Fluid Mech.* **2003**, *484*, 69-83.

(29) Bartolo, D.; Josserand, C.; Bonn, D. Singular Jets and Bubbles in Drop Impact. *Phys. Rev. Lett.* **2006**, *96*, 124501.

(30) Antonini, C.; Amirfazli, A.; Marengo, M. Drop Impact and Wettability: From Hydrophilic to Superhydrophobic Surfaces. *Phys. Fluids* **2012**, *24*, 102104.

(31) Moreira, A. L. N.; Moita, A. S.; Panão, M. R. Advances and Challenges in Explaining

Fuel Spray Impingement: How Much of Single Droplet Impact Research Is Useful? *Prog. Energy Combust. Sci.* **2010**, *36*, 554–580.

(32) Aboud, D. G. K.; Kietzig, A. M. Splashing Threshold of Oblique Droplet Impacts on Surfaces of Various Wettability. *Langmuir* **2015**, *31*, 10100–10111.

(33) Courbin, L.; Bird, J.; Stone, H. Splash and Anti-Splash: Observation and Design. *Chaos* **2006**, *16*, 041102.

(34) Zen, T.; Chou, F.; Ma, J. Ethanol Drop Impact on an Inclined Moving Surface. *Int. Commun. Heat Mass Transfer* **2010**, *37*,1025-1030.

(35) Povarov, O.; Nazarov, O.; Ignat'evskaya, L.; Nikol'Skii, A. Interaction of Drops with Boundary Layer on Rotating Surface. *J. Eng. Phys.* **1976**, *31*, 1453−1456.

(36) Chen, R. H.; Wang, H. W. Effects of Tangential Speed on Low-Normal-Speed Liquid Drop Impact on a Non-Wettable Solid Surface. *Exp. Fluids* **2005**, *39*, 754–760.

(37) Šikalo, Š.; Tropea, C.; Ganić, E. N. Impact of droplets onto inclined surfaces. *J. Colloid Interface Sci.* **2005**, *286*,661–669.

(38) *Physical Properties of Glycerine and Its Solutions*; Glycerine Producers' Association: New York, NY, **1963**.

(39) Sheely, M. L. Glycerol Viscosity Tables. *Ind. Eng. Chem.* **1932**, *24*, 1060–1064.

(40) Mao, T.; Kuhn, D. C. S.; Tran, H. Spread and Rebound of Liquid Droplets upon Impact on Flat Surfaces. *AIChE J.* **1997**, *43*, 2169–2179.

(41) Palacios, J.; Hernández, J.; Gómez, P.; Zanzi, C.; López, J. Experimental Study of Splashing Patterns and the Splashing/deposition Threshold in Drop Impacts onto Dry Smooth Solid Surfaces. *Exp. Therm. Fluid Sci.* **2013**, *44*, 571–582.

(42) Riboux, G.; Gordillo, J. Experiments of Drops Impacting a Smooth Solid Surface: A

Model of the Critical Impact Speed for Drop Splashing. *Phys. Rev. Lett.* **2014**, *113*, 024507.

(43) Ruiter, J. de; Pepper, R.; Stone, H. Thickness of the Rim of an Expanding Lamella near the Splash Threshold. *Phys. Fluids* **2010**, *22*, 022104.

(44) Allen, R. The Role of Surface Tension in Splashing. *J. Colloid Interface Sci.* **1975**, 51, 350–351.

(45) Thoroddsen, S.; Sakakibara, J. Evolution of the Fingering Pattern of an Impacting Drop. *Phys. Fluids* **1998**, *10*, 1359–1374.

(46) Marmanis, H.; Thoroddsen, S. Scaling of the Fingering Pattern of an Impacting Drop. *Phys. Fluids* **1996**, *8*, 1344, 1346.

(47) de Ruiter, J.; Lagraauw, R.; van den Ende, D.; Mugele, F. Wettability-Independent Bouncing on Flat Surfaces Mediated by Thin Air Films. *Nat. Phys.* **2014**, *11*, 48–53.

(48) Liu, Y.; Moevius, L.; Xu, X.; Qian, T.; Yeomans, J. M.; Wang, Z. Pancake Bouncing on Superhydrophobic Surfaces. *Nat. Phys.* **2014**, *10*, 515–519.

(49) Bird, J. C.; Dhiman, R.; Kwon, H.-M.; Varanasi, K. K. Reducing the Contact Time of a Bouncing Drop. *Nature* **2013**, *503*, 385–388.

(50) Gauthier, A.; Symon, S.; Clanet, C.; Quéré, D. Water Impacting on Superhydrophobic Macrotextures. *Nat. Commun.* **2015**, *6*, 8001.

(51) Liu, Y.; Andrew, M.; Li, J.; Yeomans, J. M.; Wang, Z. Symmetry Breaking in Drop Bouncing on Curved Surfaces. *Nat. Commun.* **2015**, *6*, 10034.

(52) Mangili, S.; Antonini, C.; Marengo, M.; Amirfazli, A. Understanding the Drop Impact Phenomenon on Soft PDMS Substrates. *Soft Matter* **2012**, *8*, 10045.

(53) Wildeman, S.; Visser, C. W.; Sun, C.; Lohse, D. On the Spreading of Impacting Drops.

arXiv preprint arXiv **2016**, 1602.03782.

(54) Lee, J. B.; Derome, D.; Guyer, R.; Carmeliet, J. Modeling the Maximum Spreading of Liquid Droplets Impacting Wetting and Nonwetting Surfaces. *Langmuir* **2016**, *32*, 1299–1308.

(55) Lee, J. B.; Laan, N.; de Bruin, K. G.; Skantzaris, G.; Shahidzadeh, N.; Derome, D.; Carmeliet, J.; Bonn, D. Universal Rescaling of Drop Impact on Smooth and Rough Surfaces. *J. Fluid Mech.* **2015**, *786*, R4.

(56) Scheller, B. L.; Bousfield, D. W. Newtonian Drop Impact with a Solid Surface. *AIChE J.* **1995**, *41*, 1357–1367.

(57) Roisman, I. V. Inertia Dominated Drop Collisions. II. An Analytical Solution of the Navier–Stokes Equations for a Spreading Viscous Film. *Phys. Fluids* **2009**, *21*, 52104.

(58) Clanet, C.; Béguin, C.; Richard, D.; Quéré, D. Maximal Deformation of an Impacting Drop. *J. Fluid Mech.* **2004**, *517*, 199–208.

(59) Pasandideh-Fard, M.; Qiao, Y. M.; Chandra, S.; Mostaghimi, J. Capillary Effects during Droplet Impact on a Solid Surface. *Phys. Fluids* **1996**, *8*, 650.

(60) Attané, P.; Girard, F.; Morin, V. An Energy Balance Approach of the Dynamics of Drop Impact on a Solid Surface. *Phys. Fluids* **2007**, *19*, 12101.

(61) Kim, H.-Y.; Chun, J.-H. The Recoiling of Liquid Droplets upon Collision with Solid Surfaces. *Phys. Fluids* **2001**, *13*, 643.

(62) Bechtel, S. E.; Bogy, D. B.; Talke, F. E. Impact of a Liquid Drop Against a Flat Surface. *IBM J. Res. Dev.* **1981**, *25*, 963–971.

(63) Delplanque, J. P.; Rangel, R. H. An Improved Model for Droplet Solidification on a Flat Surface. *J. Mater. Sci.* **1997**, *32*, 1519–1530.

(64) Bruce, J. W.; Giblin, P. J. *Curves and Singularities : A Geometrical Introduction to Singularity Theory* **1992**, Cambridge University Press, Cambridge, UK, Chapter 5.

Appendix A

Supporting Information for Chapter 2

A.1 Surfaces roughness details

Figure A.1 shows the profiles of the surfaces used in this study. The values of the surface descriptors are provided in Table A.1.

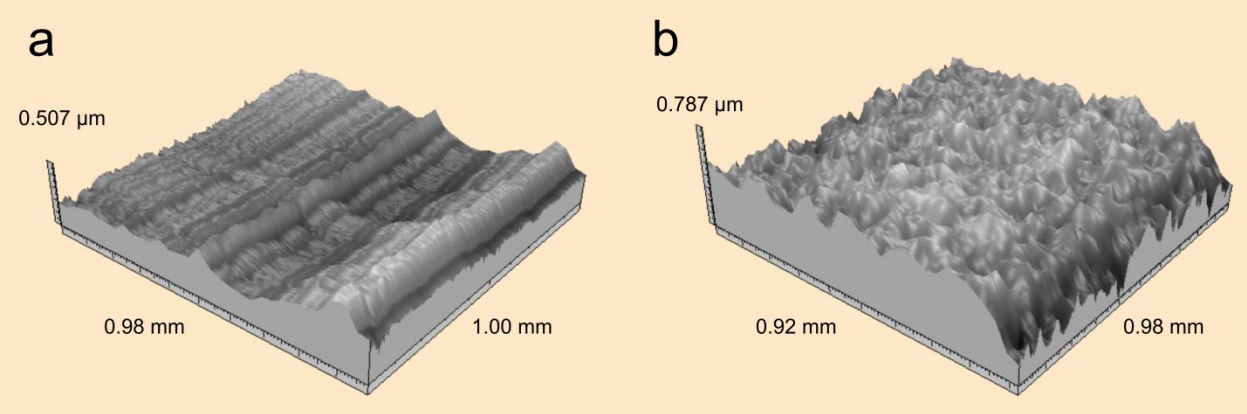

Figure A.1: Surface profielometery of the (a) stainless steel, and (b) Teflon coated stainless steel.

Table A.1: Surface descriptor values for stainless steel, and Teflon coated stainless steel.

Surface parameters	Stainless steel	Teflon coated stainless steel
Arithmetical mean height of the surface (Sa)	53±1 nm	88±15 nm
Root mean square height of the surface (Sq)	69±4 nm	112±20 nm
Maximum height of peaks (Sp)	232±45 nm	350±21 nm
Maximum height of valleys (Sv)	354±109 nm	556±102 nm
Skewness of height distribution (Ssk)	103±486	-527±287
Kurtosis of height distribution (Sku)	3736±753	3520±383

A.2 Moving surface

The assumption that the target surface is flat is justified in two ways:

First, the deviation of the surface in the frame of study is calculated using the following approach (see Figure A.2):

$$\text{Deviation } \% = \frac{\delta}{\text{X}} \times 100 \qquad (A.1)$$

where δ is the deviation of the surface from horizontal line in the frame of study (i.e. X, see Figure A.2). To calculate the largest possible deviation, the X is considered to be the largest spreading diameter measured for the range of drop velocity tested in the current work. The X was measured to be 12.06 mm. The δ is calculated using following trigonometry calculation (see Figure A.2):

$$R^2 = (R - \delta)^2 + (X/2)^2 \qquad (A.2)$$

where R is the radius of the wheel ($R = 284.5\ mm$). Using equations A.1 and A.2, the deviation percentage is found to be 0.53%, which confirms that one can consider the target surface as flat.

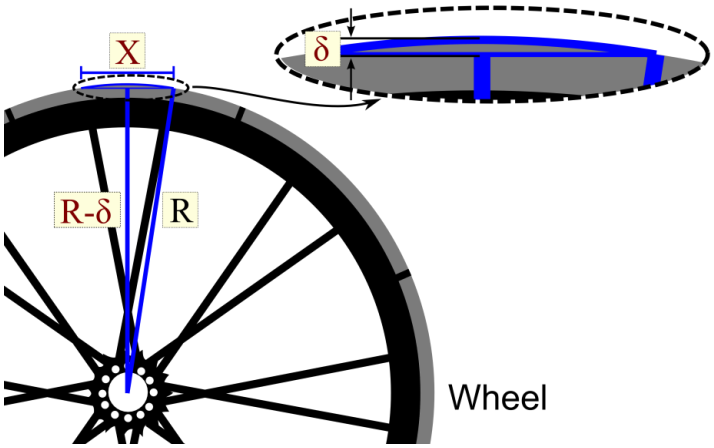

Figure A.2: Schematic view of the wheel used in this study. Zoomed view in the inset shows the deviation of the surface from horizontal line in the frame of study.

The second approach to support the assumption that the target surface is flat is as follows. As it is apparent from the experimental setup configuration (see Figures 2.2 and A.2), the surface has a curvature only in one direction, i.e. $r_1(t)$ direction in Figure A.3; there is no curvature in the direction that is perpendicular to $r_1(t)$. The perpendicular direction to $r_1(t)$ is defined as $r_2(t)$ (see Figure A.3). As such, for a given condition, the spreading radius of the drop on stationary condition are measured in both $r_1(t)$ and $r_2(t)$ directions (see Figure A.3). The results for both hydrophilic and hydrophobic surfaces, and various drop velocities ranging from 0.5 to 3.4 m/s are shown in Figure S3. The results reveal that $r_1(t)$ is equal to $r_2(t)$ for all of the conditions; this means that the drop spreads symmetric over the surface same as that of perfectly flat surface in literature [12–14]. In other words, there is no curvature effect on drop spreading.

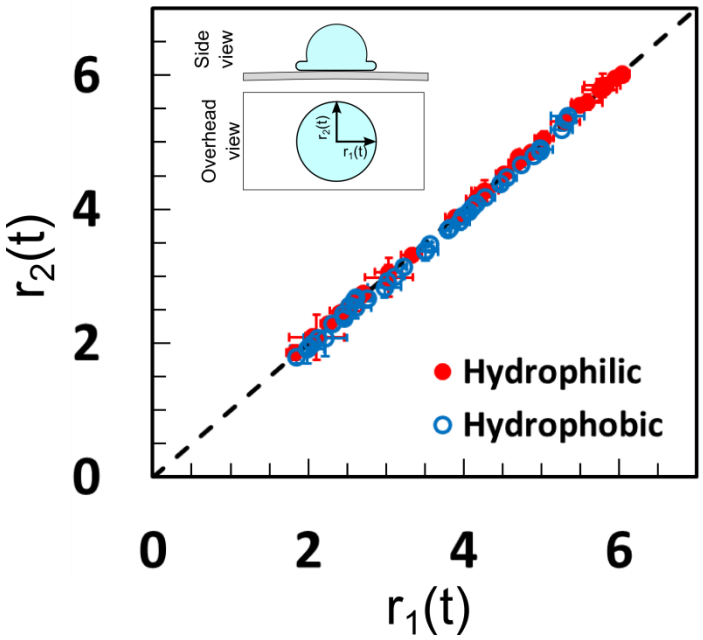

Figure A.3: Comparison of spreading radius measured in two perpendicular directions, i.e. $r_1(t)$ and $r_2(t)$; where surface has curvature only in $r_1(t)$ direction. Dashed line refers to conditions where $r_1(t)$ is equal to $r_2(t)$.

A.3 Drop impact process

Figure A.4 shows experimental results of a drop impacting onto moving hydrophilic and hydrophobic surfaces. To check the vertical movement of drop bulk, the highest surface velocity (V_s=17 m/s) and liquid viscosity (mixture 2) are considered as the extreme conditions; these conditions can have the highest possible momentum transfer from the surface to liquid. The results are provided for both highest (V_n= 3.4 m/s) and lowest drop (V_n=0.5 m/s) velocities considered in this study. As it is seen, the bulk of the drop moves only in vertical direction during impact process, which confirms that the vertical movement of drop bulk is true for all of the systems in this study.

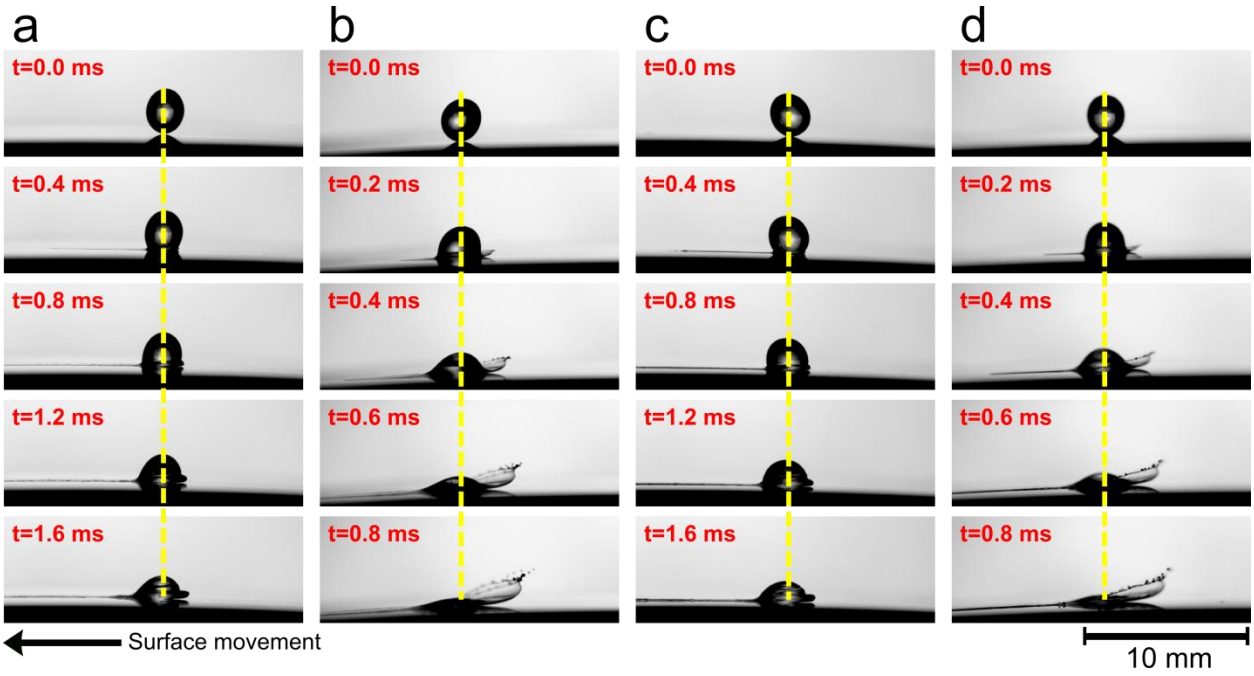

Figure A.4: Side view of the drop impact on moving (a and b) hydrophilic, and (c and d) hydrophobic surfaces. Surface velocity is V_s= 17.0 m/s and drop (mixture 2) velocities are (a and c) V_n= 0.5 m/s, and (b and d) V_n= 3.4 m/s. Vertical dashed line shows the drop apex point; apex only moves in the vertical direction. Surface moves from right to left.

A.4 Curve fitting

The experimental results which are used to determine the values of the coefficients in Eq. 2.10 are shown in Figure A.5 (symbols *). Each * symbol refers to a condition where the drop splashes azimuthally asymmetrically over the surface. The extent of the splashing (i.e. φ value) is different for each drop impact condition.

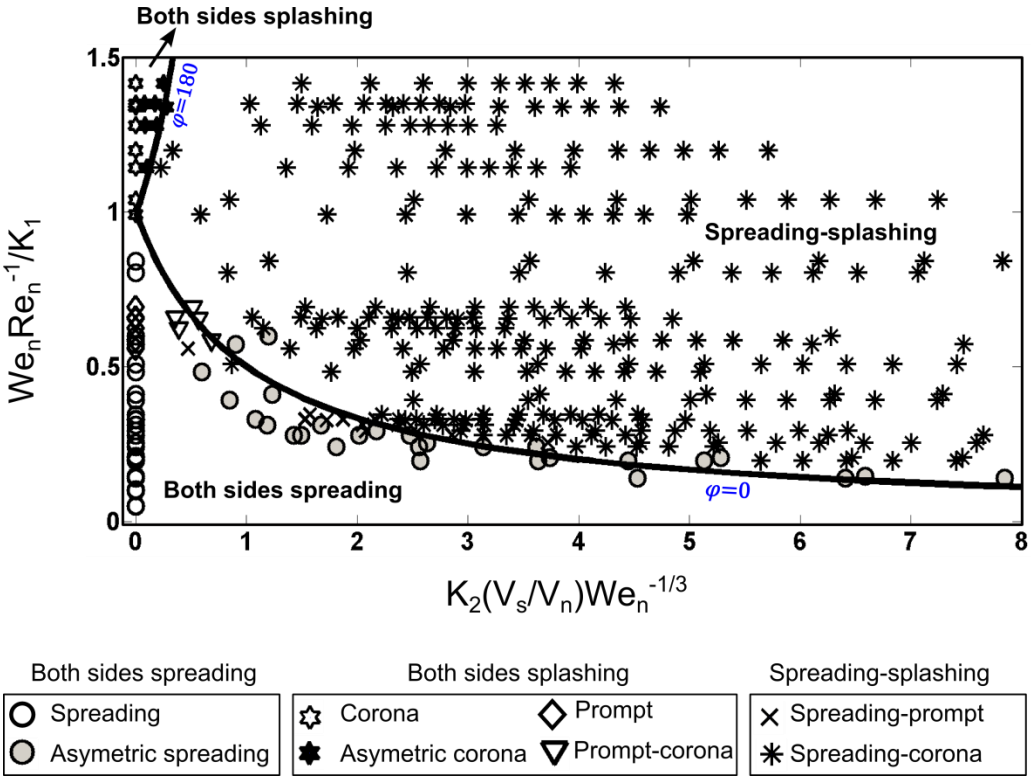

Figure A.5: Experimental data of drop impact onto moving hydrophilic and hydrophobic surfaces (symbols). The model predication (Eq. 2.10) for $\varphi = 0°$ and 180° are shown with solid lines. The line delineate spreading and splashing zones for $\varphi = 0°$ and 180°. Within the spreading-splashing regime, depending on drop impact condition, the splashing happens with different φ values.

Figure A.6 presents the experimental data of φ versus the values predicted by the developed model (Eq. 2.10). Each symbol corresponds to certain drop impact condition. The value of φ corresponding to each drop impact condition is experimentally measured (x axis in Figure A.6) and compared with the predication by Eq. 2.10 (y axis in Figure A.6). Various drop impact conditions, i.e. different drop and surface velocities, liquid viscosities, and surface wettabilities, are considered in Figure A.6. As it is shown, there is a good agreement between experimental data and the model prediction.

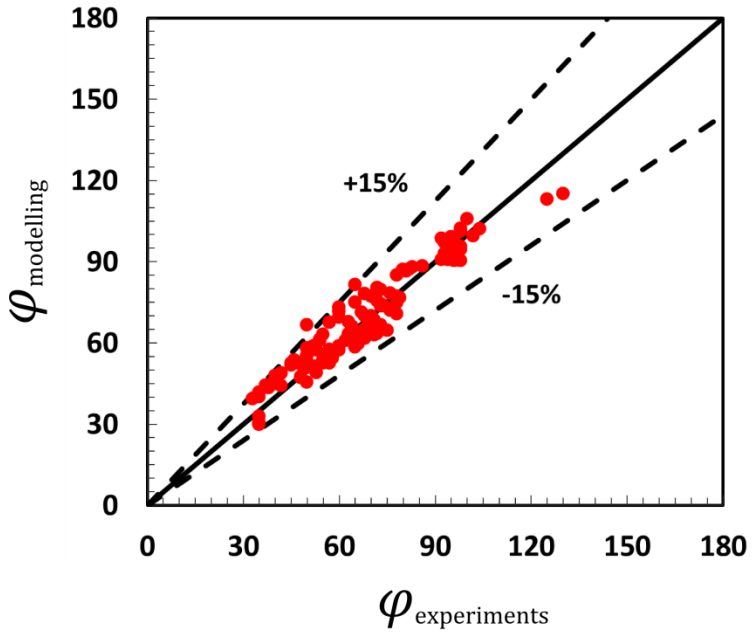

Figure A.6: Comparison of the measured φ for drop splashing with the modelling prediction (i.e. Eq. 2.10). Solid line refers to conditions where experimental data are equal to model prediction (0% deviation).

Appendix B

Supporting Information for Chapter 3

B.1 Drop spreading over a stationary surface ($\xi(t)$)

Hydrophilic surface. Figure B.1 shows time evolution of spreading factor $\xi(t)$ ($=D(t)/D$) for drop impact onto a stationary hydrophilic surface. Here, the spread factor is non-dimensionalized using maximum spread factor ξ_{max} ($=D_{max}/D_0$) and drop characteristic times is scaled using $We^{-1/4}$ [20,30]. As such, results of various drop impact conditions (i.e. various normal drop velocities and liquids), collapse onto a single curve.

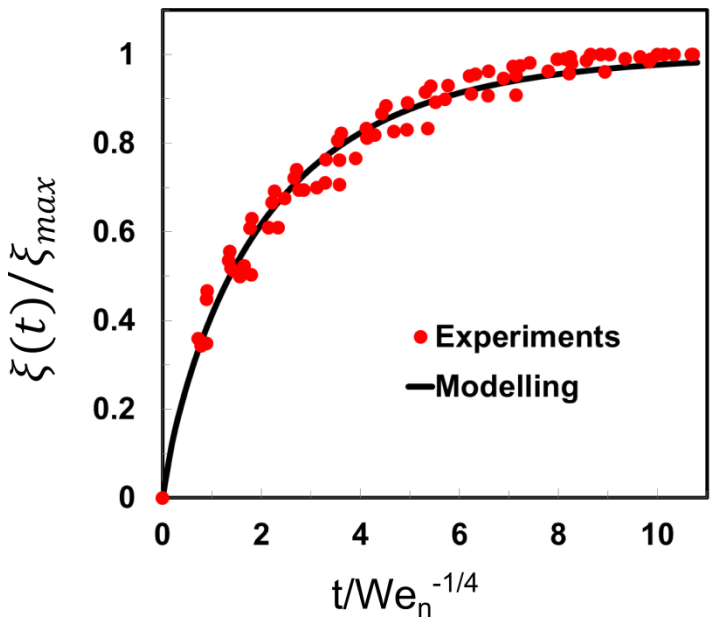

Figure B.1: Time evolution of spreading factor *ξ(t) (=D(t)/D)* for drop impact onto a stationary hydrophilic surface at various conditions of drop impact, i.e. different normal drop velocities and liquids of various viscosities. Time is in ms.

Having a single curve for all of the conditions that drop spreads over a hydrophilic surface, one can find a relation for spreading factor. As such, we consider two issues: first, the fitted curve should predict zero for the time equal to zero; and second the relation should predict the value of one for when $\xi(t) = \xi_{max}$. Considering these points, the following can be written for the hydrophilic surfaces.

$$\xi(t)/\xi_{max} = 1 - \exp\left(a\left(t/We_t^{-\frac{1}{4}}\right)^b\right) \qquad (B.1)$$

We fit the data to Eq. B.1 using the toolbox cftool in MATLAB; the fitting values were *SSE*=0.088 and R^2=0.974 which show suitable fitting process. The comparison of the experimental data versus the data from empirical correlation (B.1) is presented in Figure B.2. The result reveals the agreement between experimental data and the fitted correlation.

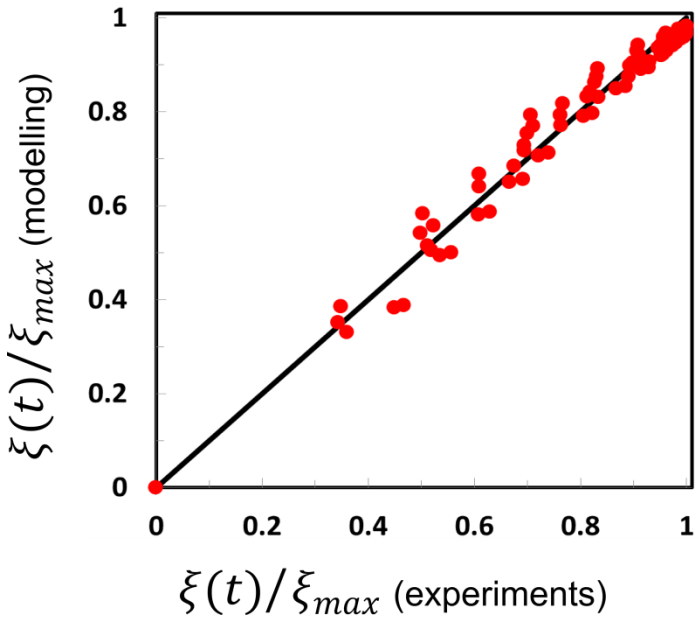

Figure B.2: Comparison of the measured $\xi(t)$ for drop spreading over a hydrophilic surface with the prediction from Eq. B.1. Solid line refers to conditions where experimental data are equal to model prediction (0% deviation).

Hydrophobic surface. Same as the hydrophilic surface, the normalized data for the hydrophobic surface is presented in Figure B.3. However, for hydrophobic surfaces, all curves collapse onto a single curve without normalizing with a characteristic time [30]. As such, considering the same points in developing a model for hydrophilic surfaces, the following relation for hydrophobic surface to predict $\xi(t)$ can be written:

$$\xi(t)/\xi_{max} = 1 - \exp(ct^d) \qquad (B.2)$$

The fitting values are found to be SSE=0.157 and R^2=0.966. Figure B.4 show results of the experimental data versus the data from empirical correlation (B.2), where there is a good agreement between experimental data and fitted correlation.

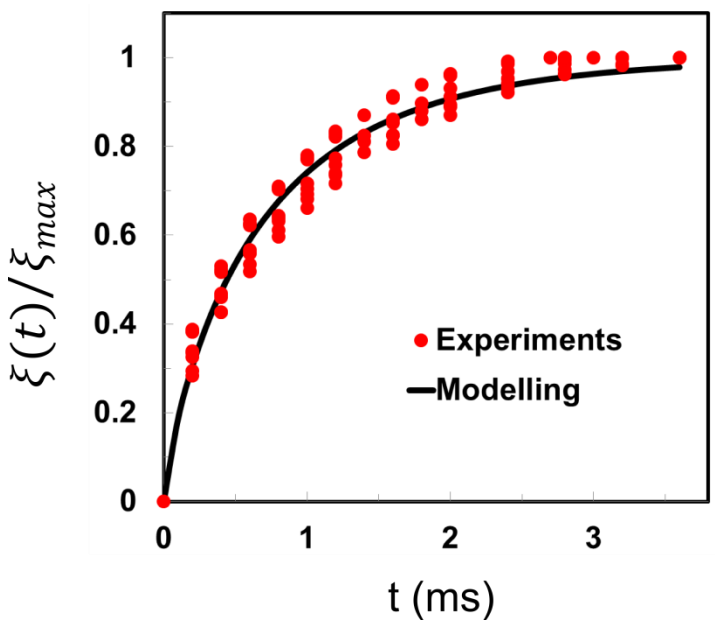

Figure B.3: Time evolution of spreading factor *ξ(t) (=D(t)/D)* for drop impact onto a stationary hydrophobic surface for different normal drop velocities and liquids of various viscosities.

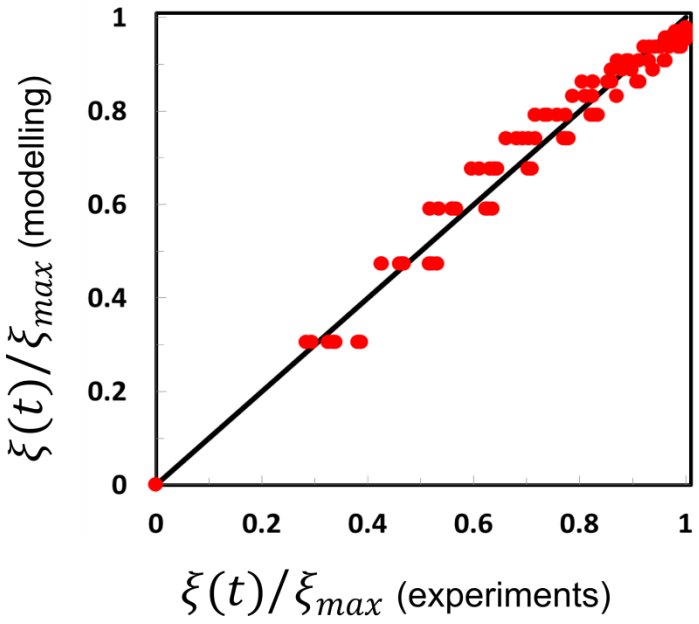

Figure B.4: Measured *ξ(t)* for drop spreading over a hydrophobic surface versus prediction from Eq. B.2. Solid line shows the conditions where experimental data are equal to model prediction (0% deviation).

B.2 Shifting factor (C)

Here we provide an empirical correlation to predict shifting factor for various conditions of the drop impact. Based on our observations, we find that the shifting factor depends on the following variables (see Figure B.5):

$$C = f(t, V_n, V_t, \mu) \qquad (B.3)$$

Note that for both hydrophilic and hydrophobic surfaces we observed the similar behavior for shifting; i.e. wettability does not have a significant effect on shifting (see Figure B.5a). This is true for all of the experimental results for all liquids.

Having the dependent variables of shifting, the question is what function links dependent variables to the shifting factor? To answer, we treated each variable separately. As such, Figure B.5a to B.5d show how shifting changes with t, V_n, V_t, and μ, respectively. Note that in each of the plots in Figure B.5, only one variable is changed and the others were kept constant. As it can be seen, shifting has a power relation with the all of dependent variables ($C = p(variable)^q$, where p and q are constants). Considering the trends of the results in Figure S5, one can expect to have $q > 1$ for Figure B.5a (C versus t), $q < 1$ for Figures B.5c (C versus V_s) and B.5d (C versus μ), and $q \approx 1$ for Figure B.5d (C versus V_n). All in all, we consider the following form for shifting:

$$C = at^b {V_n}^c {V_t}^d \mu^e \qquad (B.4)$$

where a to e are the fitting coefficients. Using the toolbox Regression in SPSS software; the values of the coefficients are found to be $a = 0.049$, $b = 1.382$, $c = 1.014$, $d = 0.701$, and $e = 0.184$; where μ is in mPa.s, time is in ms, and C is in mm. The coefficients values are in line with our expected values for q. The fitting values are *SSE*=1.161 and R^2=0.967 which show

suitable fitting process. Figure B.6 also shows agreement between experimental data and fitted correlation (Eq. B.4).

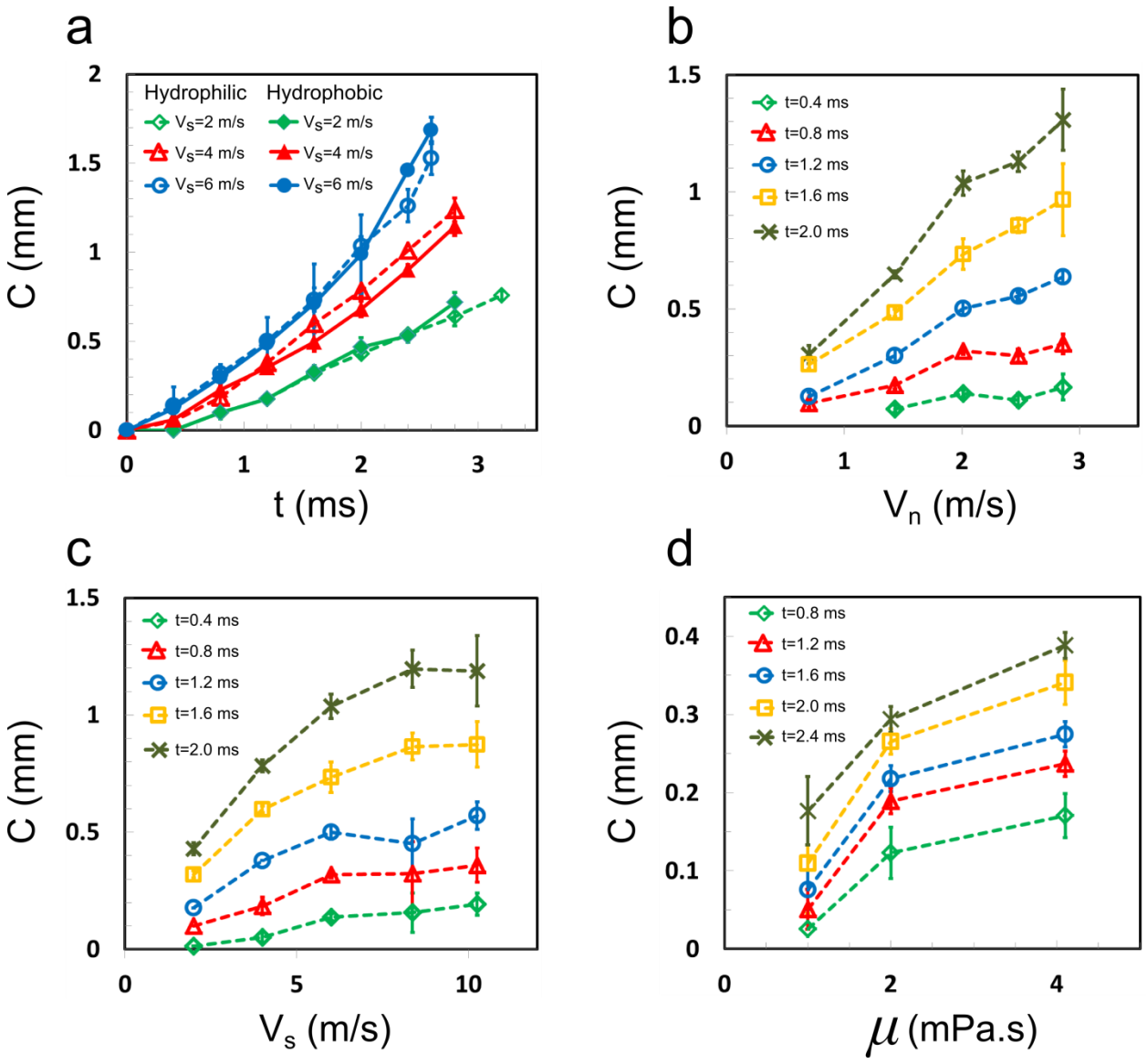

Figure B.5: Shifting factor versus (a) time, (b) normal drop velocity, (c) surface velocity, and (d) liquid viscosity. Drop impact conditions are: (a) V_n=2.01 m/s (b) V_s=6.0 m/s (c) V_n=2.01 m/s (d) V_n=0.7 m/s.

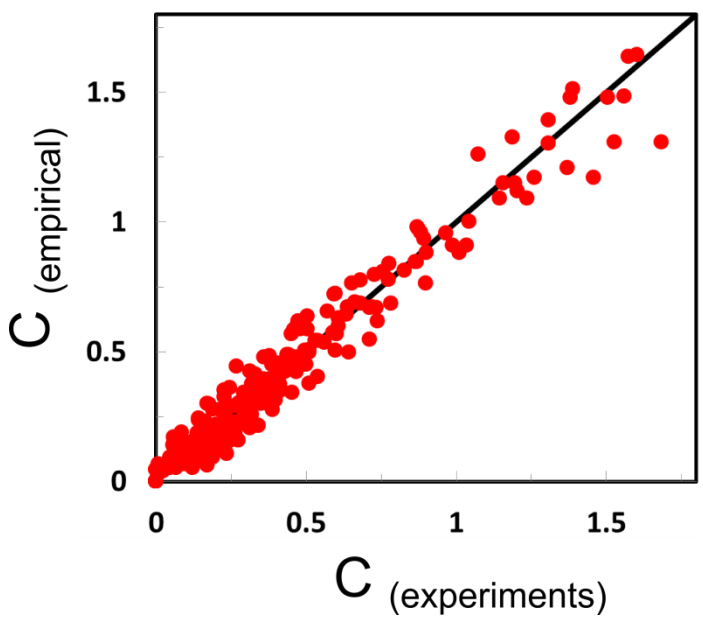

Figure B.6: Measured *C* for drop spreading versus empirical correlation prediction (Eq. B.4). Solid line shows the conditions where experimental data are equal to model prediction (0% deviation).